Journal of Archaeological Science: Reports 38 (2021) 103007

Contents lists available at ScienceDirect

Journal of Archaeological Science: Reports

journal homepage: www.elsevier.com/locate/jasrep

# A shared pottery-making tradition? Early Roman Ware 1 from Cartagena and Elche (Spain)

Miguel Angel Cau Ontiveros [a,b,c,*], Leandro Fantuzzi [b,d], Alejandro Quevedo [e,c], Evanthia Tsantini [b], Ana M. Ronda Femenía [f]

[a] ICREA, Pg. Lluís Companys 23, 08010 Barcelona, Spain
[b] Equip de Recerca Arqueològica i Arqueomètrica de la Universitat de Barcelona (ERAAUB), Institut d'Arqueologia de la Universitat de Barcelona (IAUB), Universitat de Barcelona (UB), Spain
[c] Chercheur associé, Aix-Marseille Univ, CNRS, Centre Camille Jullian, Aix-en-Provence, France
[d] Universidad de Cádiz, Spain
[e] Universidad de Murcia, Spain
[f] Museo de la Alcudia de Elche, Spain

ARTICLE INFO

*Keywords:*
Petrography
Chemistry
Cooking Wares
Roman
Provenance

ABSTRACT

The so-called Early Roman Ware 1, identified by P. Reynolds in the Alicante region, was widely distributed in the eastern part of the Iberian Peninsula. The presence of this ware in Elche (Alicante) and Valencia opened the possibility that it was widely distributed across the region. Indeed, it has been considered as a possible regional product of the area of Valencia. In Cartagena (ancient *Carthago Nova*), where our study concentrated originally, ERW1 is relatively common in 2nd and 3rd century CE contexts and has been considered as a local product. The question here is whether the ERW1 detected in Cartagena is the same as known in the Elche and Valencia regions? Were they the product of the same workshop or production center and subsequently distributed across the region? Or do we have several production centers, sharing a technological tradition but operating in different areas?

To explore this problem, we have initially characterized 29 samples from this Early Roman Ware 1 found in Cartagena (Murcia) and Elche (Alicante), using a combination of analytical techniques. WD-XRF was used for the chemical characterization, XRD for the mineralogical characterization, and, finally, optical microscopy of thin-sections was applied to investigate the petrographic features. The results of the petrographic characterization indicate the existence of a major petrographic fabric group sharing compositional features. Chemistry reveals a slightly more complex picture. One sample originates in an area of metamorphic geology, possibly in Cartagena, while the other samples, although their provenance is still unknown, most probably originated elsewhere, exploiting kaolinitic clays.

## 1. Introduction

The so-called Early Roman Ware 1 (ERW1) is a class of cooking ware typical of the southeastern Iberian Peninsula, produced from the end of the 1st century BCE until the end of the 3rd century CE. It was first identified and studied in the Vinalopó valley (Alicante) by Reynolds (1993), who proposed a typological classification consisting of nine forms, which was later extended to 18 forms (Huguet, 2012). The macroscopic characteristics, with a relatively coarse gray fabric, and the typology seem to indicate that these ceramics were kitchen items. In terms of typology, cooking pots are very common, present in various sizes, characterized by a conical body, everted rim, and umbilicated base (type ERW1.3A) often found in association with its corresponding lid. The shape repertoire includes also other variants of cooking pots and flat-base casseroles for cooking, as well as boilers which are distinguished by the presence of a carbonate concretion on their inner wall. Nevertheless, other forms like jars and containers were also produced in the same ware, covering other functions.

Other assemblages of ERW1 were published in later years, such as that found in votive wells in Llíria (Escrivà, 1995), while monographs on

* Corresponding author at: ICREA, Pg. Lluís Companys 23, 08010 Barcelona, Spain, and Departament d'Història i Arqueologia, Facultat de Geografia i Història, c/ Montalegre 6-8, 08001, Barcelona, Spain.
*E-mail address:* macau@ub.edu (M.A. Cau Ontiveros).

https://doi.org/10.1016/j.jasrep.2021.103007
Received 22 September 2020; Received in revised form 16 March 2021; Accepted 16 April 2021
Available online 6 May 2021

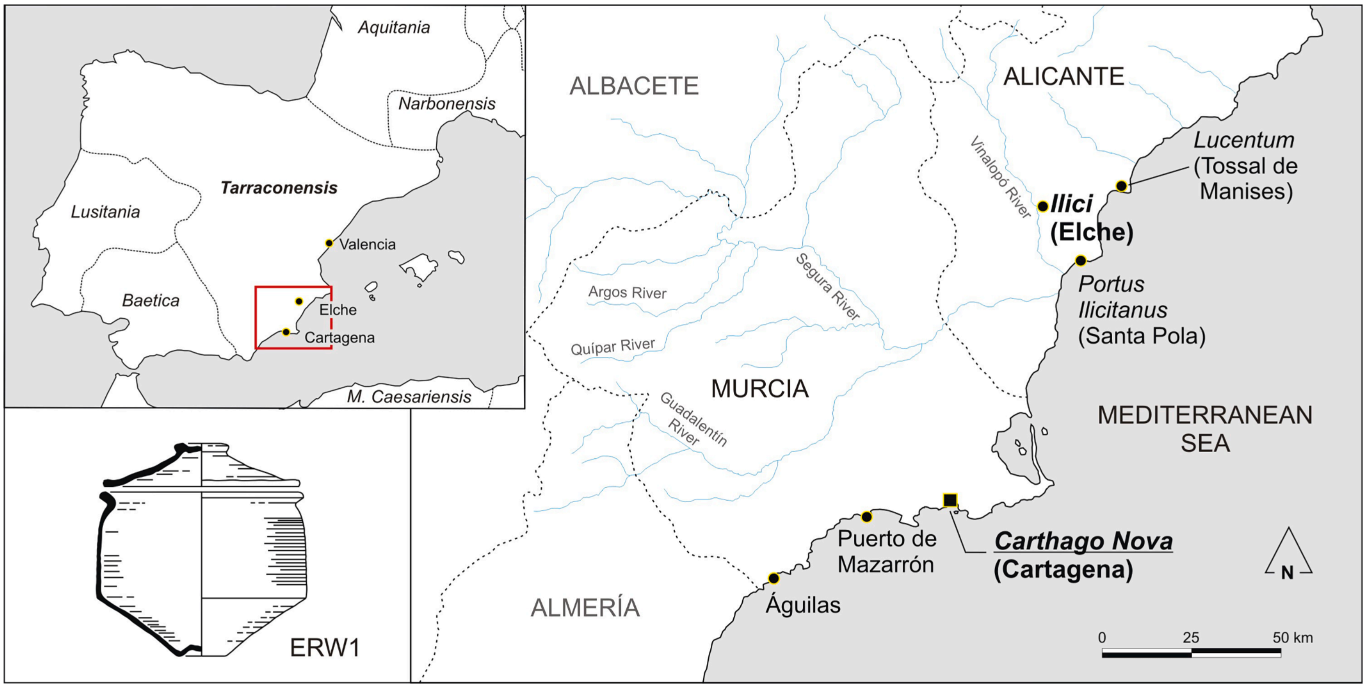


**Fig. 1.** Location of Cartagena and Elche on the eastern coast of the Iberian Peninsula and main area of distribution of ERW1 in the Iberian Peninsula.

this ware were published focused mostly on the area of Valencia (Huguet, 2012) and Cartagena (Quevedo, 2013). These works, built upon reliable stratigraphic data, widened the typological repertoire with new forms and further details of their chronology. They also helped to draw the distribution map of this ware in eastern Iberia, where it is normally abundant in Roman Imperial contexts. The distribution area of ERW1 encompasses the coast from Águilas to Sagunto, spreading inland to reach the provinces of Cuenca and Albacete. It is particularly abundant in Elche (Alicante) and Cartagena (Murcia), where it has been often interpreted as a local product (Fig. 1); it usually accounts for more than 20% of the ceramic materials from sites located inland of these two regions (Quevedo, 2015).

No kiln sites producing ERW1 have been identified so far, and the main question concerning this ware is whether all these products were manufactured in the same workshop and then distributed regionally, or if different production areas manufacturing similar ceramics could be identified, as has been suggested for the area of Valencia-Sagunto (Madrid and Buxeda, 2008; Huguet, 2012). In order to contribute to this question, a series of ERW1 ceramics from contexts found in Cartagena and comparative materials found in Elche were sampled for characterization through a combination of petrography with mineralogical and chemical analysis. The aim was to explore the variability in the assemblage and determine the provenance of the ceramics, as well as to reconstruct some aspects of their production technology. The results were also compared with previous analytical data on ERW1 and other cooking wares from the area of Valencia (Cau, 2003; Madrid and Buxeda, 2008; Cau et al., 2019a, 2019b) to explore the possibility of a provenance in this area. In summary, the ultimate goal of this paper is to gain new information on the production area/s of ERW1 cooking wares in the Roman period in this part of the Iberian Peninsula but recognizing that we are still at an initial stage of the research.

## 2. Materials and methods

A total of 29 ceramic samples were selected for analysis, including 13 samples from contexts in Cartagena (CAR-1 to CAR-13) and 16 samples found in Elche (ELX-14 to ELX-29). The selected individuals were taken from a range of forms of ERW1 (Figs. 2 and 3), all found in closed stratigraphic contexts. The samples from the Roman city of *Carthago Nova* (Cartagena) come from two rubbish dumps found at the *Fortuna Domus* (Bermejo and Quevedo, 2014) and a *domus* in Calle Jara no. 12 (Quevedo, 2015), both dated between the end of the 2nd century CE and the early 3rd century CE. In the case of Elche, the selected samples come from the archaeological site of La Alcudia, the antique city of *Ilici*. The samples come from a rubbish dump dated to the end of the first century or the first half of the second century AD covering the Augustan city wall (Tendero and Ronda, 2014a, 2014b) and from a late Roman deposit filling the baths of the Flavian period, where the ERW1 should be considered as residual material (Tendero and Ronda, 2014a, Tendero et al., 2019).

Macroscopically, samples of ERW1 cooking wares are characterized by a gray-colored matrix, sometimes very light gray to whitish, resulting from firing in a reducing-reducing atmosphere (Madrid and Buxeda, 2008; Huguet, 2012; Quevedo, 2015). A few voids and various coarse inclusions can be observed to the naked eye, the latter including glossy (quartz-like) particles of 2–3 mm, very characteristic black inclusions up to 5 mm diameter, and white (carbonate-like) inclusions also up to 5 mm and exceptionally reaching 1 cm diameter (Fig. 4). The vessels do not present any surface treatment, except for a banded polishing on the inner wall found only in some of the forms, likely to prevent food sticking during cooking.

All the ceramic samples were analyzed through optical microscopy (OM) by thin-section analysis for their petrographic and mineralogical characterization, X-ray diffraction (XRD) for further information on the mineralogical composition, and wavelength dispersive X-ray fluorescence (WD-XRF) for their chemical characterization.

The petrographic-mineralogical analysis of thin sections was performed using an Olympus BX41 polarizing microscope, working with a magnification between 20x and 200x. The ceramic fabrics were analyzed following the methodology developed by Whitbread (1989, 1995) and outlined by Quinn (2013).

For WD-XRF and XRD analyses, a sample of each specimen was powdered and homogenized in a tungsten carbide mill and dried at 100 °C for 24 h. The chemical composition of the ceramics was determined by means of WD-XRF, using a Panalytical-Axios PW 4400/40 spectrometer. Major and minor elements were determined by preparing

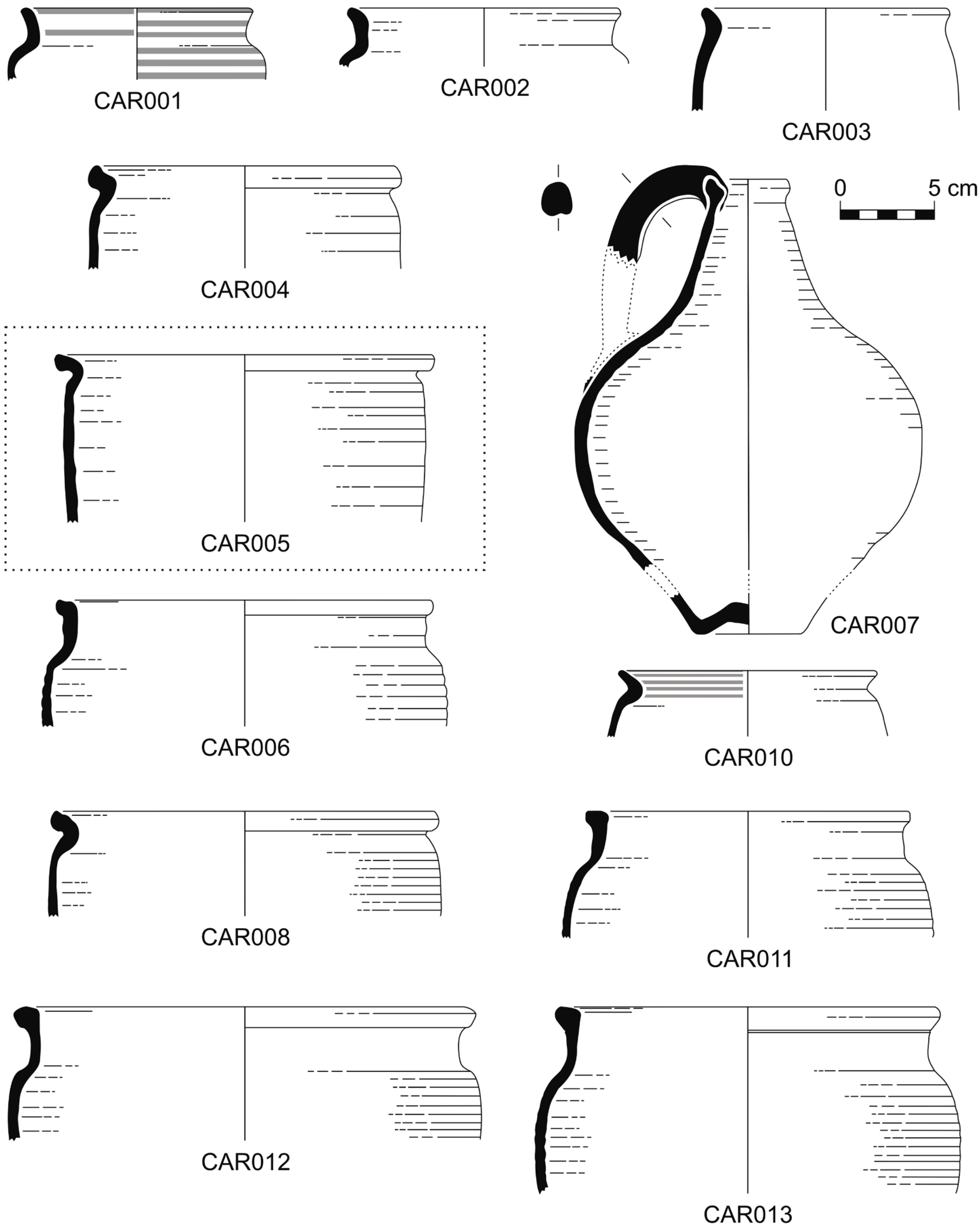


**Fig. 2.** Main types of ERW1 analyzed in this study.

duplicates of fused beads using 0.3 g of a specimen in an alkaline fusion with lithium tetraborate (1/20 solution). Trace elements and $Na_2O$ were determined using pressed powder pellets, made from 5 g of specimen mixed with an Elvacite agglutinating agent, placed over boric acid in an aluminium capsule and pressed during 60 s at 200 kN. Sixty International Geological Standards were used for calibration (Hein et al., 2002). A total of 25 major, minor, and trace elements were quantified: $Fe_2O_3$ (as total Fe), $Al_2O_3$, MnO, $P_2O_5$, $TiO_2$, MgO, CaO, $Na_2O$, $K_2O$, $SiO_2$, Ba, Rb, Mo, Th, Nb, Pb, Zr, Y, Sr, Sn, Ce, Co, Ga, V, Zn, W, Cu, and Ni. The loss on ignition (LOI) was determined by firing 0.3 g of a dried specimen, at 950 °C for 3 h. For the statistical treatment, the obtained chemical data were transformed into additive log-ratios (alr) following the methodology by Aitchison (1986, 1992) and Buxeda (1999).

The mineralogical composition was further examined through XRD analysis, carried out using 1 g of the pulverized and homogenized specimens. The measurements were taken using a PANalytical X'Pert PRO MPD alpha 1 diffractometer, working with Cu-Kα radiation (l = 1.5406 Å). Spectra were recorded from 5 to 80 °2θ, using a step-size of 0.026 °2θ and a step time of 47.5 s. The crystalline phases were examined using the software High Score Plus by PANalytical, including the Joint Committee of Powder Diffraction Standards data bank.

## 3. Regional geology

The area of Cartagena is characterized by rather complex geology. It is located in relation to the easternmost outcrops of the Alboran Domain, the Internal Zones of the Betic-Rif Arc, particularly of the Alpujárride Complex and the Nevado-Filábride Complex (Fig. 5), which are characterized by the predominance of metamorphic lithologies (Fontboté, 1983; Vera, 2004). For this reason, outcrops of micaschist, quartzite,

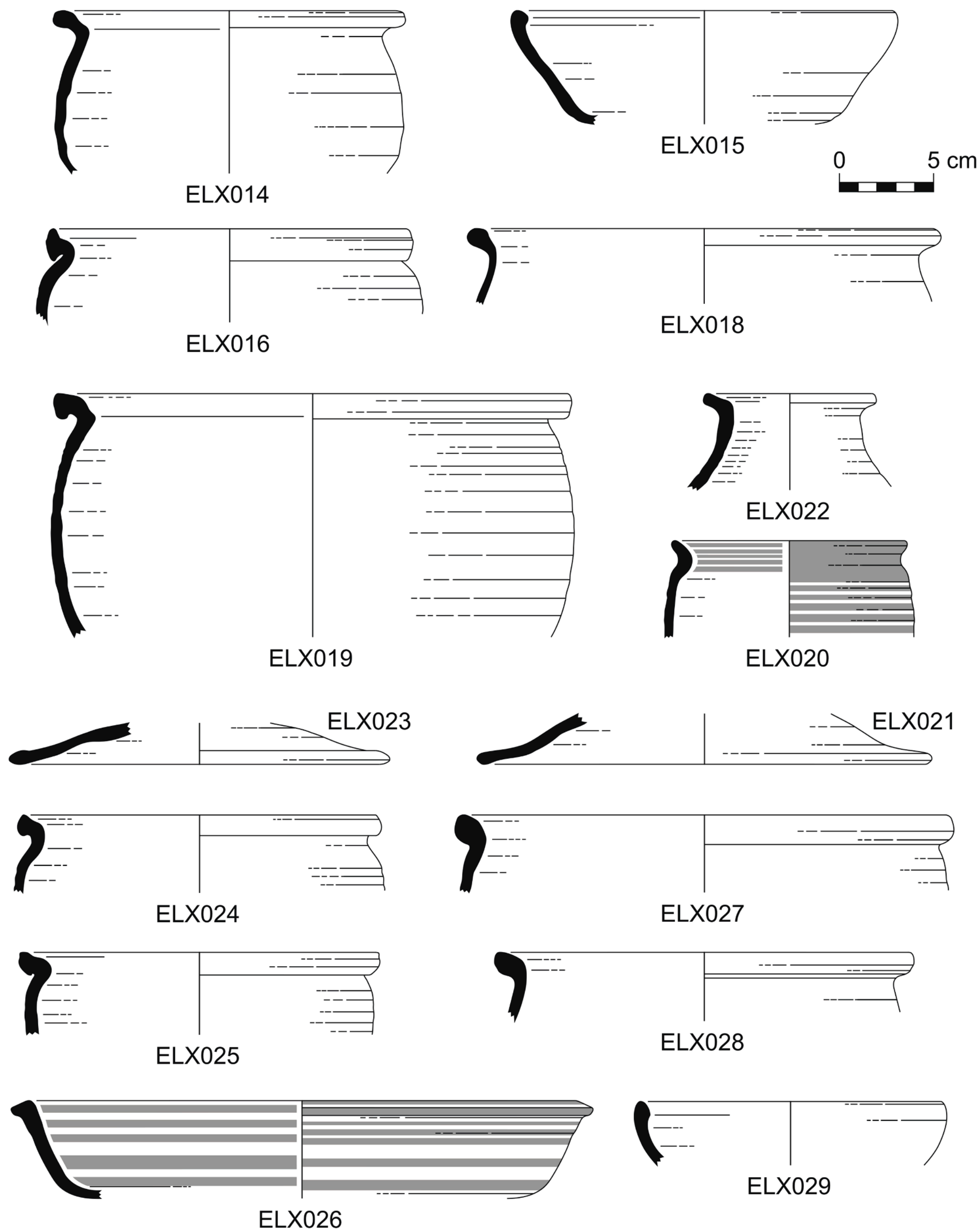


**Fig. 3.** Main types of ERW1 analyzed in this study.

gneiss, amphibolite, and marble of the Nevado-Filábride Complex, as well as phyllite, quartzite, schist, and sedimentary carbonate rocks of the Alpujárride Complex, are commonly found in the surroundings of Cartagena (Aldaya and García-Dueñas, 1972; Baena et al., 1993; Espinosa-Godoy et al., 1993). Besides this metamorphic contribution, sedimentary deposits are also widespread in the area of Cartagena, including Miocene and Pliocene marls, sands, and sandstone, and, especially, various Quaternary deposits. Rarer localized outcrops of igneous rocks —basalt, andesite, and diorite— can also be found in the surroundings of Cartagena (Fig. 5).

Elche, located 75 km north of Cartagena, differs significantly from the latter in terms of the lithologies that characterize its area. The city lies on Quaternary terrains, which largely dominate the geological landscape of the area (García-Rossell, 1973; Pignatelli et al., 1973). Post-orogenic Tertiary and Quaternary deposits, including mainly conglomerates, clays, sandstone, marls, and limestones, are particularly common in the surroundings of the city. A few kilometers to the north, other sedimentary outcrops related to the easternmost part of the External Zones (Prebetic and Subbetic) of the Alboran Domain are very widespread (García-Rossell, 1973; Pignatelli et al., 1973; Vera, 1983, 2004). Next to Elche, these consist mostly of marls, limestone, and dolomite (Fig. 5).

## 4. Results and discussion

### 4.1. OM petrographic-mineralogical results

Thin-section optical microscopy revealed that most of the samples from both Elche and Cartagena could be included in the same petrographic fabric group, 'Quartz and ferruginous argillaceous inclusions' (Fig. 6a-e), with similar fabrics in all cases. These are characterized by

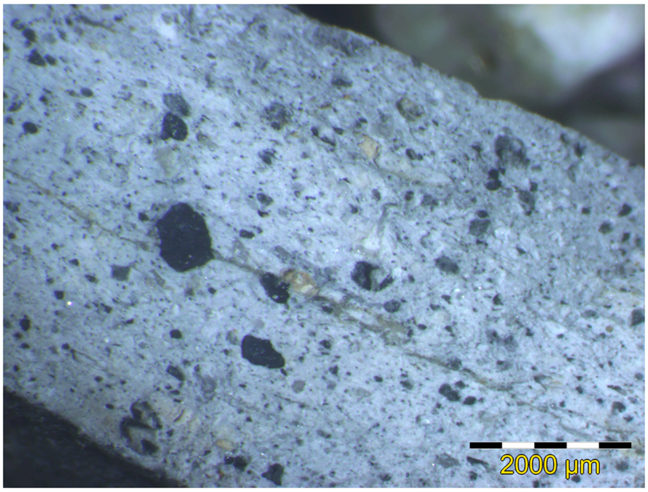


**Fig. 4.** Photograph of fresh break of an ERW1 ceramic sample, taken at 15x.

the presence of abundant inclusions, with a poorly-sorted coarse fraction (0.25–5.00 mm, mode usually between 0.30 and 0.80 mm) composed of predominant subrounded-subangular quartz, mostly monocrystalline, and variable amounts of coarse argillaceous inclusions. The latter may correspond, in most cases, to dark-colored ferruginous argillaceous rock fragments (Whitbread, 1986), although common to frequent clay pellets can also be observed. The coarse fraction can also contain very few to rare alkali feldspar, as well as accessory carbonates (micritic lumps) and quartz-sandstone fragments. The fine fraction (0.01–0.25 mm), ranging from moderately to highly abundant, is also composed of dominant quartz and frequent to common ferruginous inclusions, in addition to accessory (very few to rare) micas, feldspars, and carbonate inclusions, as well as very occasional fine grains of zircon and tourmaline. The matrix in these fabrics is generally yellowish-brown to greenish-brown (more rarely reddish-brown) under PPL, often with inhomogeneities related to core/margin color differentiation, and it ranges from optically active to inactive in XP. Voids are generally few, and mainly consist of meso-sized vughs and vesicles; elongated voids are rare, except two samples (ELX-19 and ELX-23) in which they are more common.

Based on these petrographic characteristics, the cooking wares included in this main fabric group may be associated with the use of raw clays rich in siliceous and ferruginous inclusions, and a low carbonate

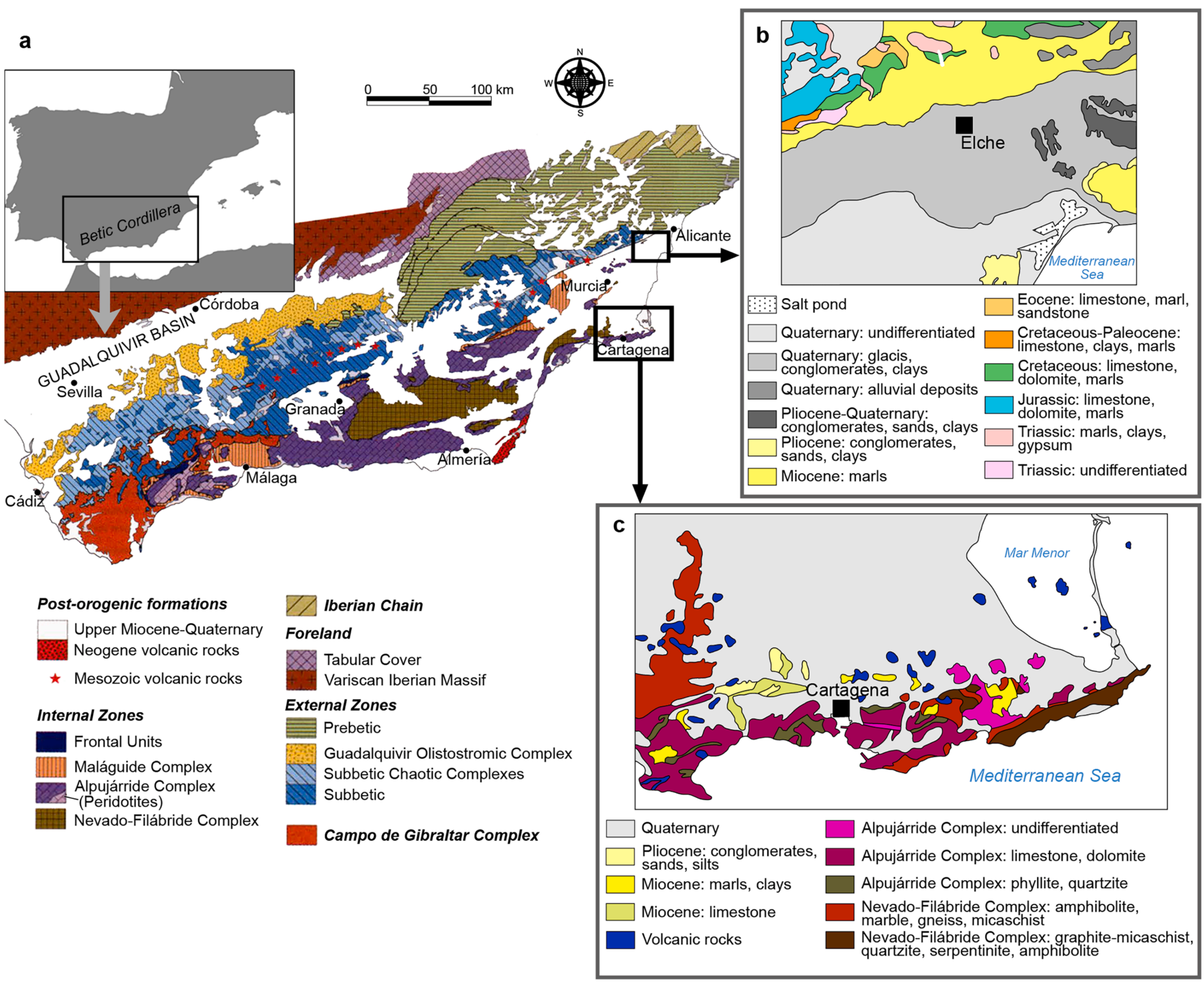


**Fig. 5.** Geological map of southeastern Spain (based on Vera 2004: fig. 4.2) with details of the areas of Cartagena (based on Aldaya and García-Dueñas 1972) and Elche (based on García-Rossell 1973).

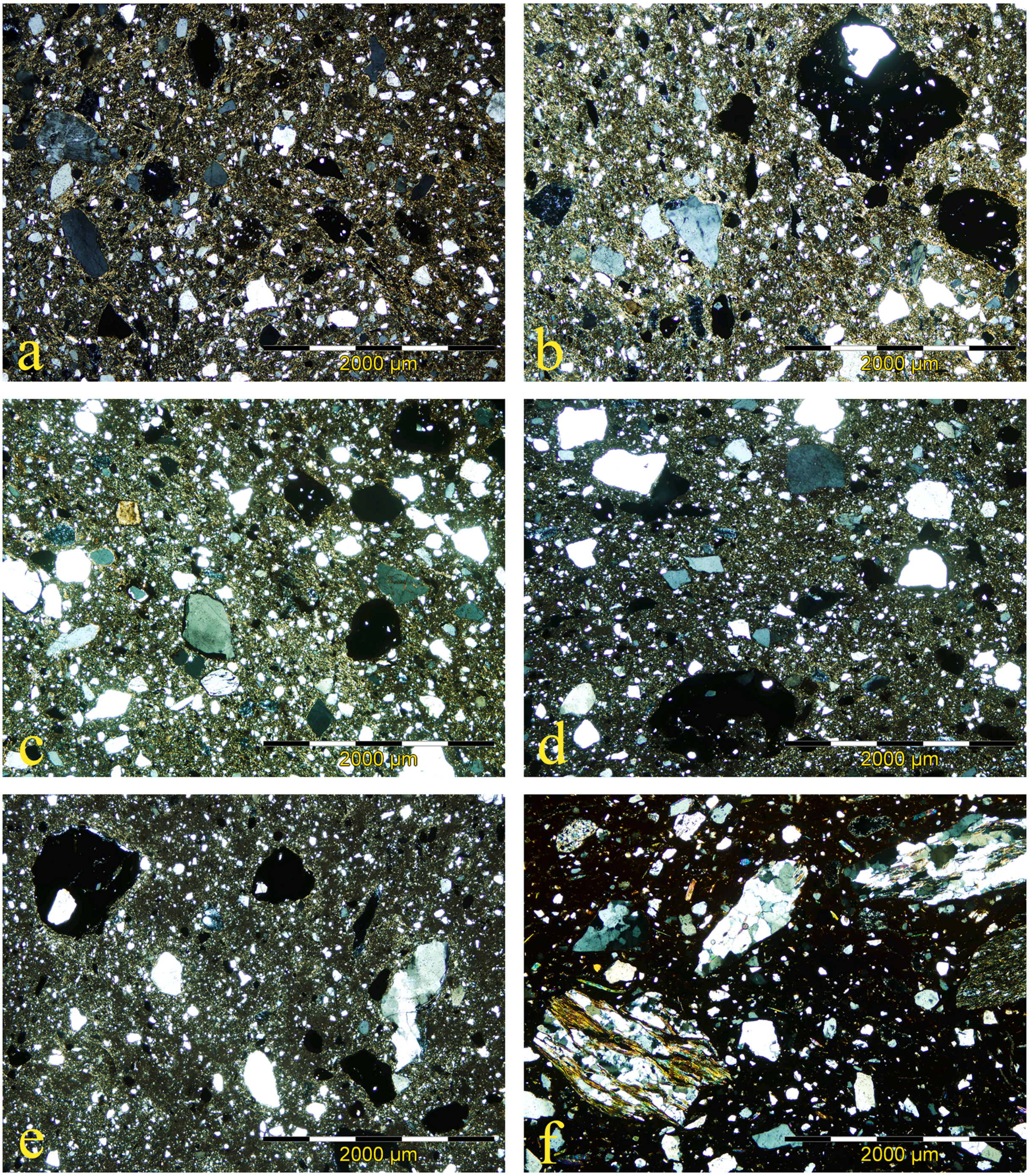


**Fig. 6.** Photomicrographs of ceramic thin sections, taken in crossed polars at 40x. 'Quartz and ferruginous argillaceous inclusions' fabric group: samples CAR-6 (a), CAR-8 (b), ELX-15 (c), ELX-19 (d), ELX-24 (e). Metamorphic fabric: sample CAR-5 (f).

content. Similarities in composition between the coarse and the fine fraction of inclusions do not allow for a clear assessment of the presence of temper in these fabrics, as the medium-coarse sandy inclusions could be interpreted either as added temper or as natural inclusions in the raw clay.

The only sample in the analyzed assemblage which does not clearly belong to the 'Quartz and ferruginous argillaceous inclusions' fabric group is CAR-5, a petrographic singleton that has a metamorphic fabric (Fig. 6f), indicating a different origin. Inclusions in this fabric are very abundant, with a predominant fine fraction, from silt and very fine sand to medium sand, composed of dominant angular-subangular quartz (both monocrystalline and polycrystalline), frequent micas (mostly muscovite), few opaques or iron oxides, plagioclase, and alkali feldspar, as well as accessory inclusions of tourmaline, zircon, amphibole, clinopyroxene, and carbonates, including very rare calcareous microfossils (globigerinids). The coarse fraction, formed by coarse sand to granules, up to 3.2 mm, is less frequent, and consists mainly of metamorphic rock fragments rich in quartz and micas, likely derived from mica-schist, containing accessory tourmaline. Less common inclusions in the coarse fraction are polycrystalline quartz, opaques or possible argillaceous rock fragments, and micritic lumps. The matrix in this fabric is optically active and shows inhomogeneities related to core/margin color differentiation, with a dark core and reddish-brown walls in PPL. Voids are common, usually as mesovughs and short elongated voids. The metamorphic contribution in

**Table 1**
Raw chemical composition of the 29 ERW1 samples analyzed in this work (WD-XRF). Major and minor elements, as well as LOI, are expressed in % of the corresponding oxide, while trace elements are expressed in parts per milion (ppm).

| | $Fe_2O_3$ | *Mn* | $TiO_2$ | *CaO* | $K_2O$ | $P_2O_5$ | $SiO_2$ | $Al_2O_3$ | *MgO* | $Na_2O$ | *Ba* | *Ce* | *Cr* | *Cu* | *Ga* | *Nb* | *Ni* | *Pb* | *Rb* | *Sr* | *Th* | *V* | *Y* | *Zn* | *Zr* | *LOI* | *SUMA* |
|---|---|---|---|---|---|---|---|---|---|---|---|---|---|---|---|---|---|---|---|---|---|---|---|---|---|---|---|
| CAR1 | 4.36 | 0.0142 | 0.98 | 0.93 | 1.64 | 0.22 | 70.37 | 16.61 | 0.52 | 0.27 | 0.0125 | 0.0332 | 0.0058 | 0.0021 | 0.0023 | 0.0021 | 0.0048 | 0.0079 | 0.0044 | 0.0127 | 0.0027 | 0.0082 | 0.0092 | 0.0041 | 0.0626 | 3.10621 | 99.17 |
| CAR2 | 6.15 | 0.0080 | 1.50 | 0.78 | 0.52 | 0.15 | 67.28 | 21.27 | 0.43 | 0.13 | 0.0444 | 0.0062 | 0.0070 | 0.0034 | 0.0031 | 0.0031 | 0.0018 | 0.0082 | 0.0032 | 0.0086 | 0.0034 | 0.0118 | 0.0044 | 0.0019 | 0.0560 | 2.79461 | 101.16 |
| CAR3 | 6.86 | 0.0091 | 1.25 | 0.73 | 2.10 | 0.14 | 68.28 | 20.11 | 0.89 | 0.12 | 0.0220 | 0.0086 | 0.0061 | 0.0023 | 0.0029 | 0.0027 | 0.0021 | 0.0049 | 0.0103 | 0.0081 | 0.0028 | 0.0106 | 0.0043 | 0.0027 | 0.0426 | 1.72300 | 102.32 |
| CAR4 | 5.91 | 0.0069 | 1.32 | 0.83 | 0.60 | 0.06 | 73.47 | 16.54 | 0.43 | 0.08 | 0.0066 | 0.0079 | 0.0068 | 0.0011 | 0.0025 | 0.0028 | 0.0016 | 0.0049 | 0.0035 | 0.0049 | 0.0033 | 0.0091 | 0.0043 | 0.0008 | 0.0656 | 0.92593 | 100.26 |
| CAR5 | 9.38 | 0.0406 | 1.29 | 1.55 | 2.44 | 0.11 | 62.29 | 18.09 | 1.26 | 1.41 | 0.0539 | 0.0080 | 0.0101 | 0.0015 | 0.0026 | 0.0021 | 0.0044 | 0.0101 | 0.0126 | 0.0152 | 0.0012 | 0.0149 | 0.0032 | 0.0081 | 0.0249 | 3.27923 | 101.28 |
| CAR6 | 3.53 | 0.0108 | 1.08 | 0.97 | 1.61 | 0.13 | 69.80 | 18.90 | 0.57 | 0.41 | 0.0128 | 0.0150 | 0.0067 | 0.0020 | 0.0025 | 0.0022 | 0.0033 | 0.0062 | 0.0044 | 0.0101 | 0.0025 | 0.0087 | 0.0056 | 0.0033 | 0.0560 | 3.15405 | 100.30 |
| CAR7 | 7.93 | 0.0095 | 1.48 | 0.99 | 0.51 | 0.04 | 68.39 | 19.93 | 0.55 | 0.12 | 0.0068 | 0.0055 | 0.0076 | 0.0018 | 0.0031 | 0.0031 | 0.0020 | 0.0056 | 0.0024 | 0.0077 | 0.0031 | 0.0123 | 0.0038 | 0.0014 | 0.0498 | 0.67272 | 100.72 |
| CAR8 | 7.08 | 0.0095 | 1.21 | 0.91 | 1.52 | 0.13 | 67.95 | 17.79 | 0.59 | 0.23 | 0.0502 | 0.0090 | 0.0067 | 0.0031 | 0.0026 | 0.0025 | 0.0025 | 0.0101 | 0.0050 | 0.0097 | 0.0025 | 0.0117 | 0.0045 | 0.0028 | 0.0432 | 2.59612 | 100.16 |
| CAR9 | 3.80 | 0.0108 | 1.14 | 1.01 | 1.24 | 0.06 | 72.20 | 19.33 | 0.60 | 0.08 | 0.0164 | 0.0102 | 0.0066 | 0.0010 | 0.0024 | 0.0023 | 0.0031 | 0.0044 | 0.0047 | 0.0076 | 0.0028 | 0.0080 | 0.0040 | 0.0018 | 0.0616 | 0.89434 | 100.48 |
| CAR10 | 7.90 | 0.0151 | 0.97 | 2.04 | 3.75 | 0.10 | 61.70 | 20.08 | 1.33 | 0.23 | 0.0334 | 0.0070 | 0.0062 | 0.0026 | 0.0029 | 0.0021 | 0.0025 | 0.0075 | 0.0175 | 0.0111 | 0.0021 | 0.0106 | 0.0029 | 0.0053 | 0.0289 | 2.28879 | 100.51 |
| CAR11 | 7.31 | 0.0097 | 1.38 | 1.34 | 1.08 | 0.07 | 62.31 | 20.72 | 0.59 | 0.25 | 0.0297 | 0.0050 | 0.0082 | 0.0014 | 0.0031 | 0.0028 | 0.0026 | 0.0106 | 0.0036 | 0.0107 | 0.0026 | 0.0127 | 0.0036 | 0.0024 | 0.0401 | 3.08725 | 98.28 |
| CAR12 | 7.47 | 0.0112 | 0.98 | 0.75 | 2.94 | 0.12 | 67.80 | 17.61 | 1.31 | 0.17 | 0.0343 | 0.0072 | 0.0086 | 0.0021 | 0.0025 | 0.0019 | 0.0022 | 0.0063 | 0.0111 | 0.0099 | 0.0015 | 0.0119 | 0.0031 | 0.0047 | 0.0277 | 1.80517 | 101.07 |
| CAR13 | 8.57 | 0.0088 | 1.30 | 0.84 | 0.85 | 0.11 | 66.60 | 21.16 | 0.60 | 0.08 | 0.0119 | 0.0073 | 0.0071 | 0.0008 | 0.0030 | 0.0027 | 0.0027 | 0.0064 | 0.0044 | 0.0078 | 0.0027 | 0.0120 | 0.0039 | 0.0019 | 0.0430 | 1.12957 | 101.35 |
| ELX14 | 6.75 | 0.0052 | 1.41 | 0.81 | 0.94 | 0.09 | 64.02 | 19.64 | 0.46 | 0.54 | 0.0161 | 0.0045 | 0.0070 | 0.0025 | 0.0028 | 0.0028 | 0.0020 | 0.0091 | 0.0018 | 0.0084 | 0.0029 | 0.0114 | 0.0037 | 0.0019 | 0.0447 | 5.73716 | 100.50 |
| ELX15 | 6.42 | 0.0084 | 1.27 | 2.09 | 0.80 | 0.07 | 68.84 | 17.83 | 0.60 | 0.20 | 0.0450 | 0.0062 | 0.0068 | 0.0012 | 0.0026 | 0.0027 | 0.0021 | 0.0075 | 0.0038 | 0.0125 | 0.0028 | 0.0103 | 0.0038 | 0.0015 | 0.0487 | 2.40202 | 100.66 |
| ELX16 | 8.24 | 0.0083 | 1.41 | 1.03 | 0.83 | 0.06 | 62.12 | 23.04 | 0.64 | 0.50 | 0.0131 | 0.0152 | 0.0078 | 0.0021 | 0.0032 | 0.0029 | 0.0026 | 0.0095 | 0.0035 | 0.0115 | 0.0027 | 0.0128 | 0.0046 | 0.0019 | 0.0397 | 1.53584 | 99.51 |
| ELX17 | 7.40 | 0.0065 | 1.64 | 0.74 | 0.49 | 0.06 | 65.70 | 22.53 | 0.48 | 0.21 | 0.0063 | 0.0063 | 0.0076 | 0.0020 | 0.0033 | 0.0033 | 0.0019 | 0.0125 | 0.0024 | 0.0099 | 0.0035 | 0.0121 | 0.0045 | 0.0015 | 0.0522 | 0.95816 | 100.32 |
| ELX18 | 7.57 | 0.0137 | 1.26 | 1.83 | 0.80 | 0.06 | 67.68 | 20.02 | 0.81 | 0.09 | 0.0106 | 0.0122 | 0.0072 | 0.0018 | 0.0025 | 0.0025 | 0.0049 | 0.0072 | 0.0036 | 0.0086 | 0.0021 | 0.0110 | 0.0050 | 0.0018 | 0.0429 | 1.01833 | 101.26 |
| ELX19 | 6.93 | 0.0055 | 1.56 | 0.74 | 0.56 | 0.05 | 68.61 | 19.73 | 0.42 | 0.41 | 0.0070 | 0.0052 | 0.0086 | 0.0021 | 0.0029 | 0.0032 | 0.0027 | 0.0094 | 0.0014 | 0.0053 | 0.0031 | 0.0138 | 0.0040 | 0.0013 | 0.0547 | 2.33860 | 101.46 |
| ELX20 | 7.61 | 0.0090 | 1.05 | 1.58 | 2.12 | 0.07 | 65.68 | 19.54 | 1.08 | 0.24 | 0.0782 | 0.0051 | 0.0061 | 0.0012 | 0.0027 | 0.0022 | 0.0022 | 0.0050 | 0.0086 | 0.0098 | 0.0023 | 0.0109 | 0.0030 | 0.0032 | 0.0316 | 1.72977 | 100.85 |
| ELX21 | 6.61 | 0.0059 | 0.98 | 1.73 | 2.54 | 0.12 | 65.98 | 19.08 | 1.17 | 0.30 | 0.0254 | 0.0065 | 0.0076 | 0.0068 | 0.0028 | 0.0020 | 0.0022 | 0.0112 | 0.0116 | 0.0105 | 0.0020 | 0.0109 | 0.0027 | 0.0043 | 0.0335 | 2.47492 | 101.10 |
| ELX22 | 5.18 | 0.0055 | 1.29 | 1.55 | 0.76 | 0.08 | 69.39 | 17.71 | 0.64 | 0.48 | 0.0189 | 0.0043 | 0.0069 | 0.0024 | 0.0026 | 0.0027 | 0.0019 | 0.0139 | 0.0021 | 0.0122 | 0.0027 | 0.0114 | 0.0032 | 0.0016 | 0.0426 | 3.10847 | 100.29 |
| ELX23 | 7.94 | 0.0072 | 1.33 | 1.32 | 0.73 | 0.10 | 66.72 | 19.10 | 0.60 | 0.44 | 0.0436 | 0.0058 | 0.0074 | 0.0030 | 0.0028 | 0.0027 | 0.0020 | 0.0067 | 0.0028 | 0.0111 | 0.0028 | 0.0107 | 0.0041 | 0.0018 | 0.0454 | 2.73607 | 101.16 |
| ELX24 | 7.35 | 0.0065 | 1.62 | 0.69 | 0.40 | 0.06 | 66.25 | 22.32 | 0.44 | 0.22 | 0.0107 | 0.0070 | 0.0078 | 0.0018 | 0.0032 | 0.0033 | 0.0020 | 0.0087 | 0.0026 | 0.0067 | 0.0036 | 0.0121 | 0.0045 | 0.0012 | 0.0533 | 1.55475 | 101.02 |
| ELX25 | 6.76 | 0.0119 | 1.49 | 0.59 | 0.65 | 0.04 | 65.62 | 23.26 | 0.80 | 0.22 | 0.0101 | 0.0040 | 0.0090 | 0.0020 | 0.0030 | 0.0029 | 0.0042 | 0.0051 | 0.0033 | 0.0068 | 0.0023 | 0.0119 | 0.0041 | 0.0016 | 0.0457 | 0.72333 | 100.27 |
| ELX26 | 6.49 | 0.0038 | 1.38 | 0.71 | 1.22 | 0.14 | 65.01 | 20.84 | 0.41 | 0.44 | 0.0090 | 0.0046 | 0.0080 | 0.0017 | 0.0030 | 0.0028 | 0.0023 | 0.0202 | 0.0022 | 0.0084 | 0.0027 | 0.0128 | 0.0033 | 0.0014 | 0.0398 | 3.54422 | 100.28 |
| ELX27 | 6.91 | 0.0071 | 1.44 | 1.19 | 0.87 | 0.09 | 68.60 | 19.76 | 0.55 | 0.23 | 0.0083 | 0.0081 | 0.0072 | 0.0014 | 0.0029 | 0.0030 | 0.0019 | 0.0052 | 0.0042 | 0.0079 | 0.0032 | 0.0104 | 0.0044 | 0.0013 | 0.0542 | 1.44065 | 101.19 |
| ELX28 | 4.99 | 0.0046 | 1.27 | 0.76 | 0.52 | 0.05 | 70.76 | 16.31 | 0.44 | 0.75 | 0.0067 | 0.0046 | 0.0064 | 0.0015 | 0.0024 | 0.0026 | 0.0018 | 0.0169 | 0.0018 | 0.0105 | 0.0027 | 0.0111 | 0.0033 | 0.0009 | 0.0529 | 4.14374 | 100.10 |
| ELX29 | 5.20 | 0.0078 | 1.50 | 0.43 | 0.65 | 0.04 | 67.02 | 22.77 | 0.84 | 0.41 | 0.0065 | 0.0045 | 0.0088 | 0.0022 | 0.0027 | 0.0027 | 0.0040 | 0.0134 | 0.0023 | 0.0072 | 0.0022 | 0.0109 | 0.0038 | 0.0021 | 0.0443 | 1.53641 | 100.50 |

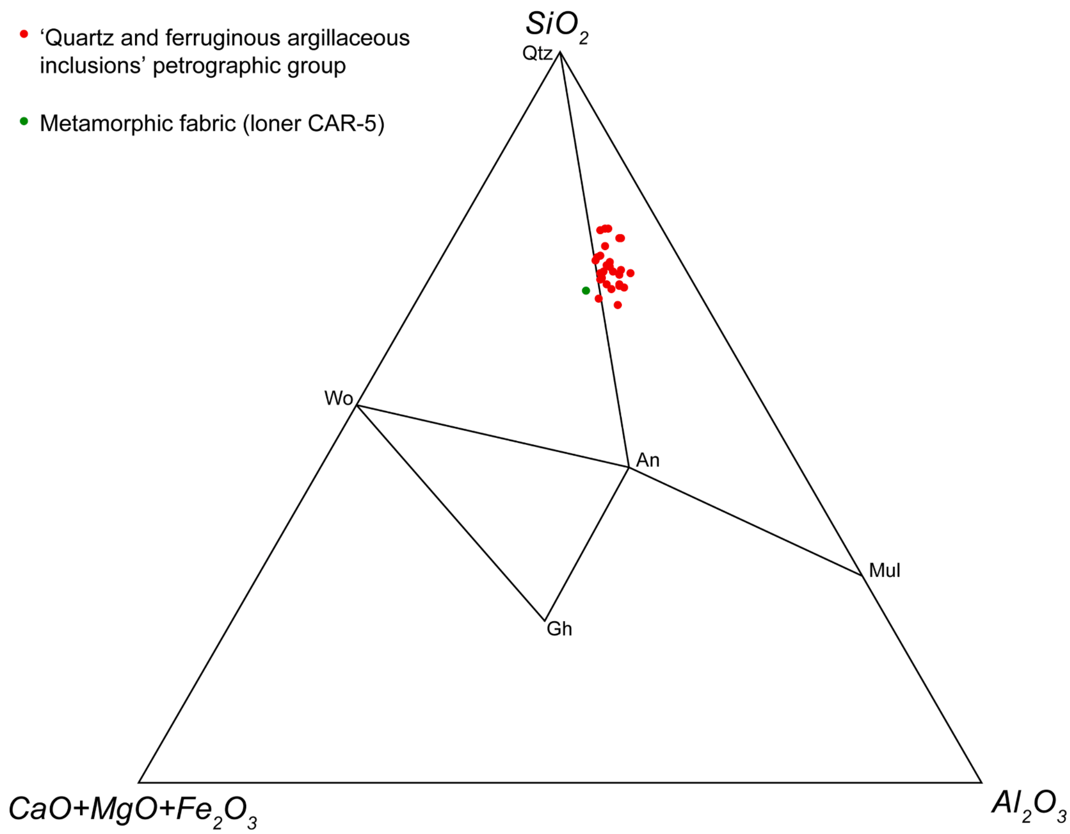


**Fig. 7.** Ceramic phase diagram for [CaO + MgO + $Fe_2O_3$]-$Al_2O_3$-$SiO_2$, with indication of the 29 ERW1 samples analyzed. Abbreviations for minerals (Kretz 1983): qtz, quartz; wo, wollastonite; an, anorthite; mul, mullite; gh, gehlenite.

sample CAR-5 found in Cartagena strongly suggests a local provenance, considering the abundance of metamorphic deposits in this area and, on the contrary, its complete absence in the area of Elche. Fabrics rich in coarse metamorphic inclusions have been commonly reported in Late Roman cooking wares produced in the area of Cartagena (Cau, 2003; Macias and Cau, 2012), usually composed of phyllitic inclusions but, in other cases, with dominant schist fragments like in CAR-5 (e.g., Fabric 1.1c in Cau, 2003). These Late Roman fabrics are not exactly the same as that found in the Early Roman sample CAR-5, but this might be related to the use of slightly different raw clay deposits and/or paste recipes in both periods.

### *4.2. WD-XRF chemical results*

The raw chemical composition of the 29 ceramic samples analyzed through WD-XRF is given in Table 1. A first assessment of these data reveals that all 28 cooking ware samples forming the petrographic fabric group 'Quartz and ferruginous argillaceous inclusions' are generally characterized by a low calcareous composition (Ca $\leq$ 2 wt% in all cases), with high content of $Al_2O_3$ (16–23 wt%) and $SiO_2$ (62–73 wt%), low MgO (0.4–1.3 wt%), and very low MnO ($\leq$0.02 wt%), while $Fe_2O_3$ concentrations are rather variable (3.5–8.6 wt%) (Table 1). This particular composition is reflected in the ceramic phase diagram for [CaO + MgO + $Fe_2O_3$]-$Al_2O_3$-$SiO_2$ (Fig. 7) (Heimann, 1989), in which most of the samples of this petrographic group fall into the thermodynamic equilibrium triangle of quartz-anorthite-mullite. On the other hand, sample CAR-5, which was a petrographic singleton, shows several particularities in the elemental composition, such as a higher content of $Fe_2O_3$, $Na_2O$, MnO, V, Zn, Cr, and Sr than the rest of the analyzed samples (Table 1); due to its higher $Fe_2O_3$ percentage, this sample behaves differently in the ceramic phase diagram falling into the thermodynamic equilibrium triangle of quartz- wollastonite-anorthite (Fig. 7).

To better explore the variability of this data set we calculated the compositional variation matrix (CVM) (Aitchison, 1986, 1992; Buxeda, 1999), which yielded a very high total variation value (vt = 3.43) indicative of a polygenic sample (Buxeda and Kilikoglou, 2003) (Table 2). According to the CVM, there are nine elements that explain more than 50% of the variability in this data set (Ba, $Na_2O$, Rb, $K_2O$, Ce, Zn, Pb, Cu, and $P_2O_5$). The variations in some of these elements, especially in $P_2O_5$, $Na_2O$, Pb, and Cu, should be taken with caution since they may be associated with possible contamination problems, for this reason, these four elements were excluded from the multivariate statistical treatment of the data.

A first grouping of the samples was obtained through a cluster analysis (CA), after an additive log-ratio (alr) transformation of the concentrations obtained by WD-XRF (Aitchison, 1986, 1992; Buxeda, 1999). The resulting cluster tree (Fig. 8) shows the presence of two main clusters or groups, CAR + ELX1 and CAR + ELX2, each composed of samples from both Cartagena and Elche (Table 3), while samples CAR-1, with anomalous high Ce (Table 1), and CAR-5 behave as chemical loners.

Further details of the chemical variability of the data set were obtained through a principal component analysis (PCA), performed on the same alr transformed subcomposition as the CA, but excluding the loners CAR-1 and CAR-5. The first principal component, PC1, is dominated by Rb, Ba, $K_2O$, Zn, and MgO, whereas PC2 is largely dominated by Ba. The biplot of PC1-PC2 (Fig. 9) illustrates the variations related to these elements. It can be observed that the samples included in the chemical group CAR + ELX1 tend to show lower PC1 scores, broadly related to higher concentrations of Rb, $K_2O$, MgO, Ba, and Zn, compared with group CAR + ELX2 (Tables 1 and 3), although for Ba and Zn there are a few samples in the latter group which also present relatively high concentrations.

In any case, a more thorough examination of these two chemical groups reveals high variability in both cases. Calculation of CVM for the small group CAR + ELX1 (n = 5) yields a vt = 0.99, which is still high

**Table 2**
Compositional variation matrix for the 29 ERW1 samples analyzed by WD-XRF.

| | $Fe_2O_3$ | $Al_2O_3$ | MnO | $P_2O_5$ | $TiO_2$ | MgO | CaO | $Na_2O$ | $K_2O$ | $SiO_2$ | Ba | Rb | Th | Nb | Pb | Zr | Y | Sr | Ce | Ga | V | Zn | Cu | Ni | Cr |
|---|---|---|---|---|---|---|---|---|---|---|---|---|---|---|---|---|---|---|---|---|---|---|---|---|---|
| *$Fe_2O_3$* | 0.00 | 0.05 | 0.24 | 0.28 | 0.06 | 0.14 | 0.17 | 0.56 | 0.41 | 0.07 | 0.55 | 0.40 | 0.14 | 0.06 | 0.21 | 0.18 | 0.15 | 0.11 | 0.33 | 0.04 | 0.03 | 0.30 | 0.23 | 0.17 | 0.05 |
| *$Al_2O_3$* | 0.05 | 0.00 | 0.20 | 0.24 | 0.02 | 0.14 | 0.19 | 0.53 | 0.42 | 0.02 | 0.63 | 0.45 | 0.06 | 0.02 | 0.16 | 0.07 | 0.07 | 0.09 | 0.24 | 0.00 | 0.02 | 0.31 | 0.18 | 0.10 | 0.02 |
| *MnO* | 0.24 | 0.20 | 0.00 | 0.31 | 0.24 | 0.16 | 0.25 | 0.56 | 0.32 | 0.18 | 0.63 | 0.34 | 0.36 | 0.26 | 0.39 | 0.30 | 0.21 | 0.16 | 0.24 | 0.22 | 0.20 | 0.19 | 0.39 | 0.09 | 0.16 |
| *$P_2O_5$* | 0.28 | 0.24 | 0.31 | 0.00 | 0.30 | 0.30 | 0.30 | 0.68 | 0.26 | 0.21 | 0.47 | 0.36 | 0.30 | 0.29 | 0.35 | 0.30 | 0.21 | 0.17 | 0.23 | 0.24 | 0.25 | 0.22 | 0.26 | 0.29 | 0.26 |
| *$TiO_2$* | 0.06 | 0.02 | 0.24 | 0.30 | 0.00 | 0.23 | 0.24 | 0.52 | 0.56 | 0.03 | 0.72 | 0.58 | 0.04 | 0.00 | 0.15 | 0.05 | 0.07 | 0.13 | 0.30 | 0.01 | 0.02 | 0.42 | 0.22 | 0.14 | 0.02 |
| *MgO* | 0.14 | 0.14 | 0.16 | 0.30 | 0.23 | 0.00 | 0.17 | 0.61 | 0.17 | 0.15 | 0.43 | 0.16 | 0.34 | 0.24 | 0.35 | 0.34 | 0.27 | 0.13 | 0.34 | 0.16 | 0.15 | 0.12 | 0.25 | 0.15 | 0.14 |
| *CaO* | 0.17 | 0.19 | 0.25 | 0.30 | 0.24 | 0.17 | 0.00 | 0.64 | 0.33 | 0.17 | 0.41 | 0.34 | 0.27 | 0.23 | 0.35 | 0.29 | 0.26 | 0.11 | 0.32 | 0.18 | 0.19 | 0.29 | 0.32 | 0.25 | 0.20 |
| *$Na_2O$* | 0.56 | 0.53 | 0.56 | 0.68 | 0.52 | 0.61 | 0.64 | 0.00 | 0.79 | 0.53 | 0.98 | 1.05 | 0.68 | 0.55 | 0.31 | 0.68 | 0.63 | 0.39 | 0.83 | 0.52 | 0.45 | 0.61 | 0.51 | 0.55 | 0.46 |
| *$K_2O$* | 0.41 | 0.42 | 0.32 | 0.26 | 0.56 | 0.17 | 0.33 | 0.79 | 0.00 | 0.39 | 0.41 | 0.10 | 0.63 | 0.56 | 0.60 | 0.63 | 0.50 | 0.29 | 0.42 | 0.43 | 0.42 | 0.10 | 0.45 | 0.38 | 0.42 |
| *$SiO_2$* | 0.07 | 0.02 | 0.18 | 0.21 | 0.03 | 0.15 | 0.17 | 0.53 | 0.39 | 0.00 | 0.61 | 0.43 | 0.05 | 0.03 | 0.17 | 0.05 | 0.05 | 0.08 | 0.21 | 0.02 | 0.03 | 0.31 | 0.19 | 0.10 | 0.02 |
| *Ba* | 0.55 | 0.63 | 0.63 | 0.47 | 0.72 | 0.43 | 0.41 | 0.98 | 0.41 | 0.61 | 0.00 | 0.40 | 0.80 | 0.72 | 0.83 | 0.86 | 0.75 | 0.43 | 0.81 | 0.62 | 0.59 | 0.36 | 0.63 | 0.70 | 0.63 |
| *Rb* | 0.40 | 0.45 | 0.34 | 0.36 | 0.58 | 0.16 | 0.34 | 1.05 | 0.10 | 0.43 | 0.40 | 0.00 | 0.67 | 0.59 | 0.76 | 0.68 | 0.55 | 0.36 | 0.46 | 0.45 | 0.46 | 0.15 | 0.53 | 0.45 | 0.45 |
| *Th* | 0.14 | 0.06 | 0.36 | 0.30 | 0.04 | 0.34 | 0.27 | 0.68 | 0.63 | 0.05 | 0.80 | 0.67 | 0.00 | 0.02 | 0.23 | 0.02 | 0.07 | 0.18 | 0.28 | 0.05 | 0.09 | 0.54 | 0.26 | 0.23 | 0.10 |
| *Nb* | 0.06 | 0.02 | 0.26 | 0.29 | 0.00 | 0.24 | 0.23 | 0.55 | 0.56 | 0.03 | 0.72 | 0.59 | 0.02 | 0.00 | 0.16 | 0.04 | 0.07 | 0.13 | 0.29 | 0.01 | 0.03 | 0.43 | 0.22 | 0.16 | 0.03 |
| *Pb* | 0.21 | 0.16 | 0.39 | 0.35 | 0.15 | 0.35 | 0.35 | 0.31 | 0.60 | 0.17 | 0.83 | 0.76 | 0.23 | 0.16 | 0.00 | 0.25 | 0.25 | 0.16 | 0.47 | 0.16 | 0.13 | 0.46 | 0.23 | 0.27 | 0.15 |
| *Zr* | 0.18 | 0.07 | 0.30 | 0.30 | 0.05 | 0.34 | 0.29 | 0.68 | 0.63 | 0.05 | 0.86 | 0.68 | 0.02 | 0.04 | 0.25 | 0.00 | 0.04 | 0.19 | 0.22 | 0.07 | 0.11 | 0.53 | 0.28 | 0.18 | 0.10 |
| *Y* | 0.15 | 0.07 | 0.21 | 0.21 | 0.07 | 0.27 | 0.26 | 0.63 | 0.50 | 0.05 | 0.75 | 0.55 | 0.07 | 0.07 | 0.25 | 0.04 | 0.00 | 0.13 | 0.11 | 0.07 | 0.10 | 0.37 | 0.25 | 0.10 | 0.09 |
| *Sr* | 0.11 | 0.09 | 0.16 | 0.17 | 0.13 | 0.13 | 0.11 | 0.39 | 0.29 | 0.08 | 0.43 | 0.36 | 0.18 | 0.13 | 0.16 | 0.19 | 0.13 | 0.00 | 0.22 | 0.09 | 0.08 | 0.18 | 0.20 | 0.14 | 0.09 |
| *Ce* | 0.33 | 0.24 | 0.24 | 0.23 | 0.30 | 0.34 | 0.32 | 0.83 | 0.42 | 0.21 | 0.81 | 0.46 | 0.28 | 0.29 | 0.47 | 0.22 | 0.11 | 0.22 | 0.00 | 0.26 | 0.30 | 0.33 | 0.41 | 0.19 | 0.27 |
| *Ga* | 0.04 | 0.00 | 0.22 | 0.24 | 0.01 | 0.16 | 0.18 | 0.52 | 0.43 | 0.02 | 0.62 | 0.45 | 0.05 | 0.01 | 0.16 | 0.07 | 0.07 | 0.09 | 0.26 | 0.00 | 0.01 | 0.32 | 0.18 | 0.13 | 0.02 |
| *V* | 0.03 | 0.02 | 0.20 | 0.25 | 0.02 | 0.15 | 0.19 | 0.45 | 0.42 | 0.03 | 0.59 | 0.46 | 0.09 | 0.03 | 0.13 | 0.11 | 0.10 | 0.08 | 0.30 | 0.01 | 0.00 | 0.30 | 0.18 | 0.12 | 0.01 |
| *Zn* | 0.30 | 0.31 | 0.19 | 0.22 | 0.42 | 0.12 | 0.29 | 0.61 | 0.10 | 0.31 | 0.36 | 0.15 | 0.54 | 0.43 | 0.46 | 0.53 | 0.37 | 0.18 | 0.33 | 0.32 | 0.30 | 0.00 | 0.32 | 0.23 | 0.29 |
| *Cu* | 0.23 | 0.18 | 0.39 | 0.26 | 0.22 | 0.25 | 0.32 | 0.51 | 0.45 | 0.19 | 0.63 | 0.53 | 0.26 | 0.22 | 0.23 | 0.28 | 0.25 | 0.20 | 0.41 | 0.18 | 0.18 | 0.32 | 0.00 | 0.29 | 0.19 |
| *Ni* | 0.17 | 0.10 | 0.09 | 0.29 | 0.14 | 0.15 | 0.25 | 0.55 | 0.38 | 0.10 | 0.70 | 0.45 | 0.23 | 0.16 | 0.27 | 0.18 | 0.10 | 0.14 | 0.19 | 0.13 | 0.12 | 0.23 | 0.29 | 0.00 | 0.09 |
| *Cr* | 0.05 | 0.02 | 0.16 | 0.26 | 0.02 | 0.14 | 0.20 | 0.46 | 0.42 | 0.02 | 0.63 | 0.45 | 0.10 | 0.03 | 0.15 | 0.10 | 0.09 | 0.09 | 0.27 | 0.02 | 0.01 | 0.29 | 0.19 | 0.09 | 0.00 |
| $\tau_{\cdot i}$ | 4.92 | 4.23 | 6.60 | 7.08 | 5.08 | 5.62 | 6.47 | 14.63 | 9.99 | 4.08 | 14.99 | 11.16 | 6.41 | 5.15 | 7.54 | 6.47 | 5.37 | 4.23 | 8.07 | 4.26 | 4.26 | 7.68 | 7.18 | 5.52 | 4.27 |
| vt / $\tau_{\cdot i}$ | 0.70 | 0.81 | 0.52 | 0.48 | 0.67 | 0.61 | 0.53 | 0.23 | 0.34 | 0.84 | 0.23 | 0.31 | 0.53 | 0.67 | 0.45 | 0.53 | 0.64 | 0.81 | 0.42 | 0.80 | 0.80 | 0.45 | 0.48 | 0.62 | 0.80 |
| r v.$\tau_{\cdot i}$ | 0.96 | 0.96 | 0.85 | 0.79 | 0.91 | 0.69 | 0.89 | 0.79 | 0.12 | 0.96 | 0.16 | 0.23 | 0.90 | 0.91 | 0.80 | 0.90 | 0.92 | 0.98 | 0.89 | 0.95 | 0.94 | 0.18 | 0.94 | 0.95 | 0.95 |
| vt | 3.43 | | | | | | | | | | | | | | | | | | | | | | | | |

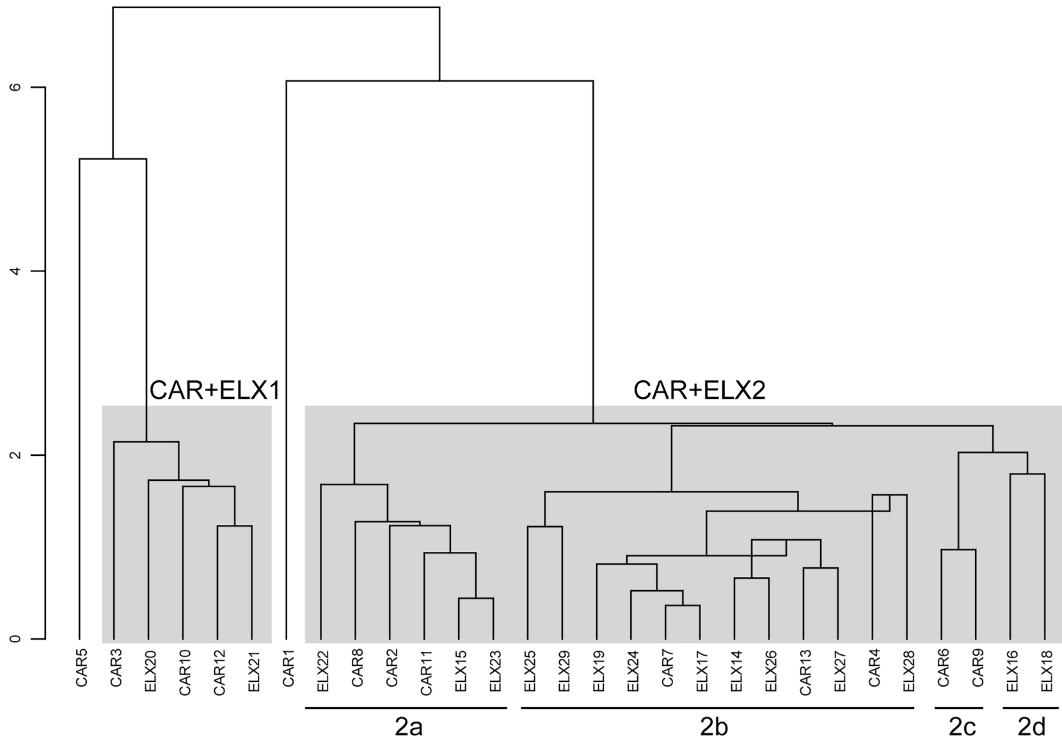


**Fig. 8.** Dendrogram resulting from cluster analysis, using the centroid agglomerative method and the squared Euclidean distance, on 29 ceramic samples, based on the subcomposition $Fe_2O_3$, $Al_2O_3$, MnO, $TiO_2$, MgO, CaO, $K_2O$, Ba, Rb, Th, Nb, Zr, Y, Sr, Ce, Ga, V, Zn, Ni, and Cr, using $SiO_2$ as divisor in the log-ratio transformation of the data. Chemical groups (CAR + ELX1 and CAR + ELX2) and sub-groups are indicated.

and most likely related to a polygenic sample. The most variable elements in this group, according to the CVM, are Ba ($\tau_i = 6.00$), and CaO ($\tau_i = 5.30$), although it can be observed that the high $\tau_i$ value for Ba is biased by the presence of a very high concentration in sample ELX-20. Recalculation of CVM after excluding Ba results in a lower vt (0.73); even if this value would be normally considered too high to be indicative of a monogenic group of ceramics (Buxeda and Kilikoglou, 2003), it should be mentioned that, in the case of coarse-grained fabrics, slightly higher vt values (always $< 1.00$) might also be found in pottery with a geochemical relation or a common origin (Buxeda et al., 2001).

Similarly, the large group CAR + ELX2 (n = 22) also shows a high vt value (1.44), and in this case most of this variability is explained by variations in Ba ($\tau_i = 10.21$) and Ce ($\tau_i = 3.99$). These are elements that dominate the subdivision of this group into four sub-groups in CA (Fig. 8): CAR + ELX2a (n = 6), with high content in Ba and low in Ce; CAR + ELX2b (n = 12), with low Ba and Ce; and finally CAR + ELX2c (n = 2) and CAR + ELX2d (n = 2), both with high Ce and low Ba, but differentiated from each other by much lower content in $Fe_2O_3$ in the former than in the latter (Table 3). The total variation observed within each of these sub-groups ($vt_{CAR+ELX2a} = 0.69$; $vt_{CAR+ELX2b} = 0.82$; $vt_{CAR+ELX2c} = 0.40$; $vt_{CAR+ELX2d} = 0.85$) might indicate broadly monogenic groups of pottery, assuming again the hypothesis that slightly high vt values could be expected in coarse-grained fabrics.

In summary, the results of the WD-XRF analysis revealed a high variability in chemical composition for the assemblage of 28 cooking wares included in the 'Quartz and ferruginous argillaceous inclusions' fabric group. Up to five chemical subgroups, each with relatively low vt, could be identified, most likely associated with various production sites or units. It must be stressed that it was not possible to correlate these differences between chemical groups or subgroups with differences in petrographic fabric in thin section and this points also towards a common general origin.

### 4.3. XRD mineralogical results

The XRD analysis of the 29 samples of cooking wares provided further information on their mineralogical composition. The mineral phases identified in each diffractogram allowed for an estimation of equivalent firing temperatures or EFT (Roberts, 1963), based on the identification of primary phases and the eventual occurrence of firing phases, in addition to secondary phases due to use or post-depositional processes (Maggetti, 1982; Cultrone et al., 2001; Cau, 2003; Buxeda and Cau, 2004; Maritan, 2004; Maggetti et al., 2011).

The 28 samples included in the main petrographic group ('Quartz and ferruginous argillaceous inclusions') show various associations of mineral phases (Table 4). The majority of these contain quartz, alkali feldspar, anatase, and, in many cases, illite-muscovite as primary phases. Illite can be found at firing temperatures up to 950 °C in non-calcareous clays (Cultrone et al., 2001), although its breakdown may occur at lower temperatures in a reducing firing atmosphere (Maritan, 2004). For this reason, the absence of illite-muscovite in other samples (Table 4) might suggest EFTs over 850/950 °C. Maghemite is very frequent (18 samples) as a firing phase (Fig. 10a), which indicates an EFT over 750 °C under reducing firing conditions (Maritan, 2004; Travé et al., 2019); on the other hand, the occurrence of hematite in very rare cases (ELX-14 and ELX-23) might correspond either to a primary phase or to a firing phase under oxidizing conditions. Only in two samples, ELX-18 and ELX-25, is it possible to observe spinel peaks in the diffractograms along with the absence of illite-muscovite, pointing to higher firing temperatures (EFT $\geq$ 950/1000 °C) (Fig. 10b). In summary, the results of XRD mineralogical analysis suggest that most of the cooking wares included in the main petrographic group were likely fired at temperatures between 750 and 950 °C under reducing conditions (Table 4), with rare samples fired at higher temperatures or under oxidizing conditions. It must be mentioned that all these samples generally show mineral associations typical of non-calcareous pottery, except for the presence of low peaks of calcite in rare cases (Table 4) which correspond to samples with slightly

**Table 3**
Mean normalized chemical composition of groups CAR + ELX1 and CAR + ELX2, as well as of the four sub-groups identified in the latter (CAR + ELX2a to CAR + ELX2d). Mean (m) and standard deviation (sd) values are given for each element.

| | $Fe_2O_3$ | $Al_2O_3$ | MnO | $P_2O_5$ | $TiO_2$ | MgO | CaO | $Na_2O$ | $K_2O$ | $SiO_2$ | Ba | Rb | Th | Nb | Pb | Zr | Y | Sr | Ce | Ga | V | Zn | Cu | Ni | Cr |
|---|---|---|---|---|---|---|---|---|---|---|---|---|---|---|---|---|---|---|---|---|---|---|---|---|---|
| CAR + ELX1 (n = 5) | | | | | | | | | | | | | | | | | | | | | | | | | |
| m | 7.35 | 19.44 | 0.01 | 0.11 | 1.05 | 1.16 | 1.38 | 0.21 | 2.71 | 66.43 | 390 | 119 | 21 | 22 | 71 | 331 | 32 | 100 | 69 | 28 | 111 | 41 | 30 | 23 | 70 |
| sd | 0.57 | 1.03 | 0.00 | 0.03 | 0.11 | 0.19 | 0.61 | 0.07 | 0.71 | 2.17 | 230 | 35 | 5 | 3 | 27 | 57 | 6 | 12 | 13 | 2 | 5 | 11 | 22 | 2 | 12 |
| CAR + ELX2 (n = 22) | | | | | | | | | | | | | | | | | | | | | | | | | |
| m | 6.67 | 20.36 | 0.01 | 0.08 | 1.40 | 0.57 | 1.02 | 0.30 | 0.84 | 68.62 | 181 | 32 | 29 | 28 | 93 | 497 | 42 | 90 | 73 | 29 | 115 | 18 | 19 | 26 | 75 |
| sd | 1.34 | 2.00 | 0.00 | 0.04 | 0.14 | 0.13 | 0.41 | 0.19 | 0.34 | 2.73 | 149 | 10 | 4 | 3 | 43 | 71 | 6 | 22 | 33 | 3 | 15 | 6 | 7 | 9 | 7 |
| CAR + ELX2a (n = 6) | | | | | | | | | | | | | | | | | | | | | | | | | |
| m | 6.85 | 19.56 | 0.01 | 0.10 | 1.36 | 0.59 | 1.36 | 0.29 | 0.92 | 68.79 | 396 | 35 | 29 | 28 | 98 | 472 | 40 | 111 | 62 | 29 | 117 | 21 | 25 | 22 | 73 |
| sd | 1.01 | 1.72 | 0.00 | 0.03 | 0.11 | 0.08 | 0.48 | 0.14 | 0.37 | 2.07 | 119 | 10 | 3 | 2 | 28 | 54 | 5 | 15 | 16 | 3 | 10 | 5 | 9 | 4 | 6 |
| CAR + ELX2b (n = 12) | | | | | | | | | | | | | | | | | | | | | | | | | |
| m | 6.85 | 20.68 | 0.01 | 0.07 | 1.47 | 0.54 | 0.79 | 0.31 | 0.70 | 68.47 | 90 | 27 | 30 | 30 | 100 | 507 | 40 | 77 | 59 | 29 | 118 | 15 | 18 | 24 | 77 |
| sd | 0.99 | 2.18 | 0.00 | 0.03 | 0.11 | 0.14 | 0.19 | 0.21 | 0.25 | 2.72 | 31 | 9 | 4 | 2 | 52 | 69 | 4 | 17 | 14 | 3 | 12 | 4 | 5 | 8 | 8 |
| CAR + ELX2c (n = 2) | | | | | | | | | | | | | | | | | | | | | | | | | |
| m | 3.72 | 19.43 | 0.02 | 0.10 | 1.13 | 0.59 | 1.00 | 0.25 | 1.45 | 72.17 | 148 | 46 | 27 | 23 | 54 | 598 | 49 | 90 | 128 | 25 | 85 | 26 | 15 | 32 | 68 |
| sd | 0.13 | 0.03 | 0.00 | 0.05 | 0.02 | 0.01 | 0.01 | 0.24 | 0.29 | 0.45 | 23 | 1 | 2 | 0 | 14 | 30 | 12 | 20 | 37 | 1 | 6 | 11 | 7 | 2 | 2 |
| CAR + ELX2d (n = 2) | | | | | | | | | | | | | | | | | | | | | | | | | |
| m | 7.98 | 21.74 | 0.02 | 0.06 | 1.35 | 0.73 | 1.44 | 0.30 | 0.82 | 65.45 | 119 | 36 | 24 | 27 | 85 | 416 | 48 | 101 | 139 | 29 | 120 | 19 | 20 | 37 | 76 |
| sd | 0.60 | 2.51 | 0.01 | 0.00 | 0.13 | 0.11 | 0.55 | 0.30 | 0.03 | 2.91 | 20 | 0 | 5 | 3 | 18 | 16 | 2 | 22 | 23 | 5 | 15 | 1 | 2 | 16 | 6 |

higher CaO, but always < 2.1 wt%, according to WD-XRF results; at least a part of this calcite might be secondary, as suggested by its presence in a sample (ELX-15) where illite-muscovite is fully decomposed, therefore indicating an EFT not lower than 900/950 °C.

On the other hand, in sample CAR-5, a petrographic loner with a metamorphic fabric, the presence of illite-muscovite as a primary phase and maghemite as a firing phase, as well as the absence of other firing phases typical of higher temperatures (e.g. spinel), suggest an EFT in the range 750–900/950 °C (Table 4).

## 5. Discussion

The analytical characterization of ERW1 from Cartagena and Elche combining chemical and minero-petrographic analysis showed that, in petrographic terms, most of the samples can be classified in a 'Quartz and ferruginous argillaceous inclusions' petrographic fabric group with strong similarities among them. The chemical analysis also showed similarities for the majority of the samples, forming a main chemical group, CAR + ELX2 (n = 23), including samples from both Cartagena and Elche. Nevertheless, five samples from this petrographic group formed another chemical group, CAR + ELX1, including three samples from Cartagena and two from Elche, mainly due to compositional differences in specific elements (higher $K_2O$, MgO, and Rb than in CAR + ELX 2). It is important to highlight that it was not possible to correlate the chemical differences between both chemical groups with differences in petrographic fabrics under thin section. Sample CAR-5 behaves as a chemical loner, in agreement with the petrographic evidence.

ERW1 samples from the cities of Valencia and Sagunto, the Roman *Valentia* and *Saguntum*, respectively, were analyzed previously by Madrid and Buxeda (2008), including 14 samples that were examined using WD-XRF and XRD, and compared to the data for Late Antique cooking wares found in excavations of *Valentia* previously studied (Cau, 2003) acting, somehow, as a control group for a possible provenance in Valencia. The results showed that only one of the samples analyzed really fell in a group containing mainly Late Roman cooking wares from Valencia that could be considered as local, while for the rest of samples the provenance was unclear (Madrid and Buxeda, 2008). In general, the latter results showed a certain complexity in the materials analyzed, prompting the conclusion that these products certainly shared a common pottery-making tradition but probably originated in different workshops. Even if the WD-XRF chemical results of that study were not published, preventing a comparison with data from the present study, the composition of the majority of the samples analyzed must be broadly similar to that of our groups CAR + ELX1 and CAR + ELX2, as they behave similarly in the ceramic phase diagram falling into the thermodynamic equilibrium triangle of quartz-anorthite-mullite (Madrid and Buxeda, 2008). Also, the XRD mineralogical composition, with common presence of anatase and maghemite (Madrid and Buxeda, 2008), reveals strong similarities with the samples analyzed here from contexts in Cartagena and Elche.

To further investigate the provenance of the ERW1 samples from Cartagena and Elche, and particularly the hypothesis of possible production in Valencia, we have compared these materials with samples from non-calcareous cooking wares found in the region of Valencia contained in the database of the ERAAUB in Barcelona, and for which a regional provenance in Valencia or its surroundings was suggested. These included Late Roman ceramics from various contexts in Valencia city (Cau, 2003; Cau et al., 2019a), as well as from the *villa* of L'Horta Vella in Bétera, in the *territorium* of *Valentia* (Cau et al., 2019b). This comparison showed that the vast majority of the regional cooking wares from the area of Valencia had a different chemical composition and formed a clearly separate group in cluster analysis (Fig. 11). This reinforces the idea that the ERW1 ceramics analyzed from Cartagena and Elche have no relationship in terms of provenance with those analyzed in the city of Valencia and the rural site in Bétera. It was, however, interesting to observe that two samples of cooking wares found in Valencia, U00017 and U00018, match very well with the main compositional group of

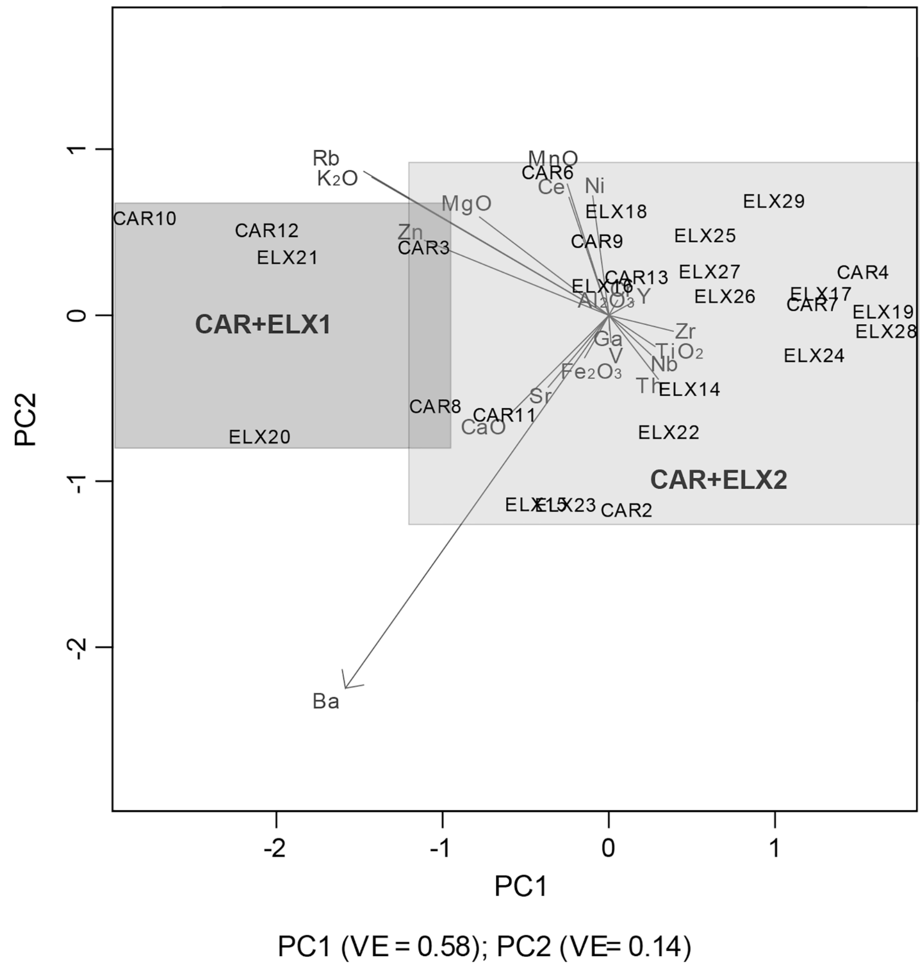


**Fig. 9.** PCA on the alr-transformed chemical data of 27 samples (excluding loners CAR-1 and CAR-5), using $SiO_2$ as divisor, based on the same sub-composition as the CA in Fig. 7. Plot of the two first principal components (PC1-PC2), which account for 58% and 14% of the total variance, respectively.

**Table 4**
Main crystalline phases detected by XRD in the 29 ceramic samples and estimation of equivalent firing temperatures (EFT). Abbreviations for minerals (Kretz 1983): Qtz, quartz; Kfs, K-feldspar; Ant, anatase; Ill-Ms, illite-muscovite; Pl, plagioclase; Cal, calcite; Mgh, maghemite; Hem, hematite; Spl, spinel.

| *Petrographic group* | *Samples* | *Mineral phases (XRD)* | | | | | | | | | *EFT (°C)* |
|---|---|---|---|---|---|---|---|---|---|---|---|
| | | *Qtz* | *Kfs* | *Ant* | *Ill-Ms* | *Pl* | *Cal* | *Mgh* | *Hem* | *Spl* | |
| Quartz and ferruginous argillaceous inclusions (n = 28) | CAR-10 | + | + | + | + | | + | | | | ≤800/850 |
| | CAR-1, CAR-6 | + | + | + | + | | | | | | ≤900/950 |
| | ELX-14 | + | + | + | + | | | | + | | |
| | ELX-21, ELX-22 | + | + | + | + | | + | + | | | 750–800/850 |
| | CAR-8, CAR-11, CAR-12, ELX-16, ELX-20, ELX-26, ELX-28 | + | + | + | + | | | + | | | 750–900/950 |
| | CAR-9, ELX-29 | + | + | + | | | | | | | ~900/950 |
| | CAR-2, CAR-3, CAR-4, CAR-7, CAR-13, ELX-17, ELX-19, ELX-24, ELX-27 | + | + | + | | | | + | | | |
| | ELX-23 | + | + | + | | | | | + | | |
| | ELX-15 | + | + | + | | | + | + | | | |
| | ELX-25 | + | + | + | | | | | | + | ≥950/1000 |
| | ELX-18 | + | + | + | | + | | | | + | |
| Loner CAR-5 (metamorphic fabric) | CAR-5 | + | + | | + | + | | + | | | 750–900/950 |

ERW1 (CAR + ELX2) (Fig. 11); these samples were classified as Fabric 6.16 by Cau (2003), which is indeed similar to the 'Quartz and ferruginous argillaceous inclusions' petrographic fabric group defined in our study. It is also worthy of note that the majority of the ERW1 samples analyzed by Madrid and Buxeda (2008) also clustered together with those two samples of Fabric 6.16, in what they called group A, so this must be equivalent to our group CAR + ELX2. Moreover, the authors also identified another group, B, characterized by higher $K_2O$, Rb, and Ba, and similar in composition to the sample U00012 (Madrid and Buxeda, 2008), as occurs with our group CAR + ELX1 (Fig. 11). In summary, it is

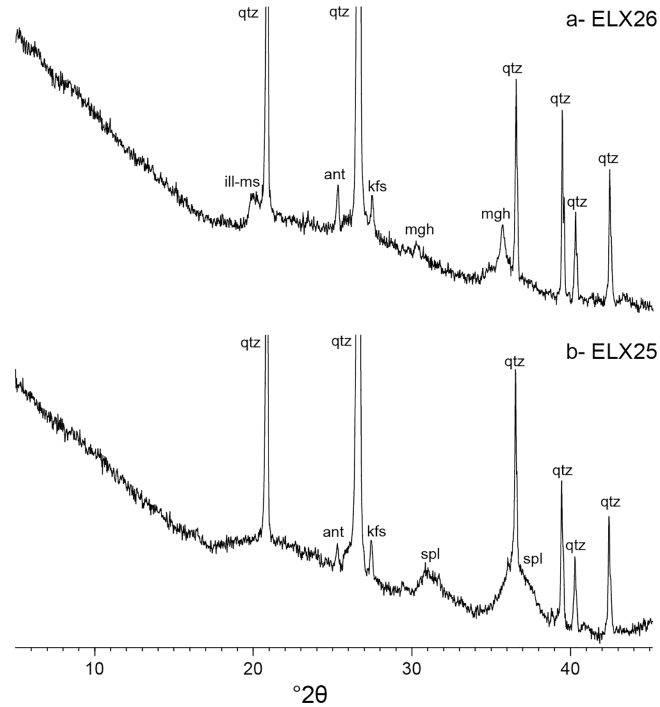


**Fig. 10.** XRD spectra of two representative ERW1 samples in the 'Quartz and ferruginous argillaceous inclusions' petrographic group, related to lower (a) and higher (b) firing temperatures. Abbreviations for minerals (Kretz 1983): qtz, quartz; kfs, K-feldspar; ant, anatase; ill-ms, illite-muscovite; mgh, maghemite; spl, spinel.

possible to observe strong compositional similarities between most of the ERW1 samples analyzed from contexts in Valencia and Sagunto (Madrid and Buxeda, 2008) and from Cartagena and Elche in the present study, suggesting a likely common provenance area (or areas), which, according to the comparison with the ERAAUB database, might not be located in Valencia or, at least, in the same source area as the regional cooking wares found in Late Roman contexts from Valencia.

For the ERW1 samples analyzed here, the lack of metamorphic inclusions points towards a provenance outside Cartagena. The petrographic-mineralogical composition may be compatible with a provenance hypothesis in the area of Elche, although other areas in Murcia or the Valencia region (to name the nearest possible sources) cannot be disregarded from a strictly geological point of view. In fact, the relatively high content of $Al_2O_3$, the presence of anatase, and maybe also the variation of some trace elements such as Ce, Th, and Y, indicate the use of alumina-rich clayey raw materials, probably kaolinitic or bauxitic, used either alone or mixed with another clay. Deposits of kaolin are common for instance in the northwestern region of Valencia. Huguet (2012) suggested a provenance in the area of Valencia-Llíria-Sagunto due to the abundant occurrence and high typological diversity of ERW1 in this area, although the same can be stated for Elche and Cartagena. In fact, other alumina-rich clays are also common in areas towards the south, including parts of Alicante and Murcia. Sampling and analysis of potential raw materials for ceramic production in the region will be necessary as reference material for comparison, in order to provide additional support to these hypotheses.

Conversely, sample CAR-5 points to the occurrence of another different ware in the ceramic assemblage of Cartagena. The composition of this singleton is compatible with the metamorphic outcrops that are frequent in the region of Cartagena (Fig. 5). If this sample can be confirmed archaeologically as ERW1, this would indicate the existence

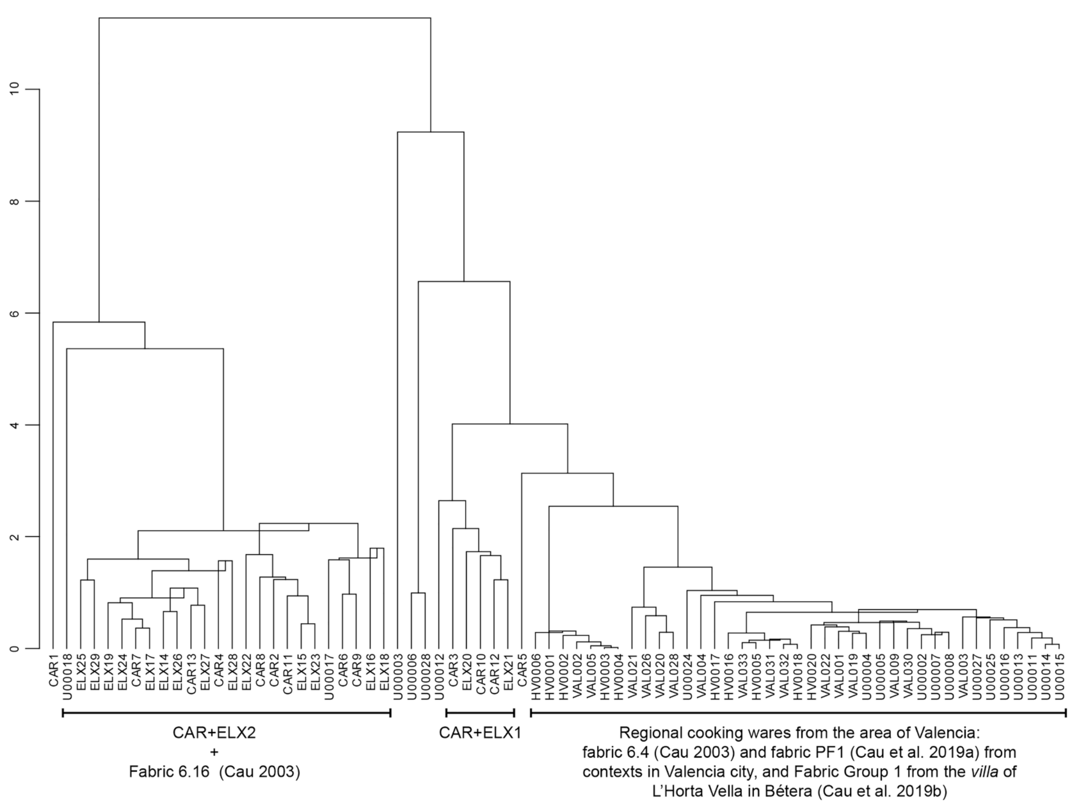


**Fig. 11.** Dendrogram resulting from cluster analysis on 74 ceramic samples, including the 29 ERW1 samples from Cartagena and Elche, as well as 45 reference samples of cooking wares from Late Roman contexts in the area of Valencia: labels U (Cau 2003), VAL (Cau et al. 2019a), and HV (Cau et al. 2019b). The analysis was performed using the centroid agglomerative method and the squared Euclidean distance, based on the sub-composition $Fe_2O_3$, $Al_2O_3$, MnO, $TiO_2$, MgO, CaO, $K_2O$, Ba, Rb, Th, Nb, Zr, Y, Sr, Ce, Ga, V, Zn, Ni, and Cr, using $SiO_2$ as divisor in the log-ratio transformation of the data.

of another production area likely located in the Cartagena region. Otherwise, this ware should probably not be classified as ERW1.

From a technological point of view, ERW1 was wheel-made using non-calcareous clayey raw materials probably of kaolinitic origin. The use of this type of clay is common in the Roman period and certainly shares a tradition with some well-known wares used in Gaul such as the kaolinitic wares (*céramique commune kaolinithique*) and the *céramique à physolites* (e.g., Pasqualini, 2009; Raynaud, 2007; Raynaud and Elie, 2006). This was a clear technological choice, as this ware (or group of wares) was conceived primarily as a cooking ware to be used in direct contact with fire, and the use of non-calcareous clays in general had advantages in terms of thermal shock resistance and heat conductivity (Hein et al., 2008; Müller et al., 2014). It is difficult to be sure, without analyzing the raw clayey materials, if the ERW1 had added temper, as the non-plastics observed could be also naturally contained in the sediments. The results concerning the firing temperature and atmosphere are also interesting. In general, there is a predominance of reducing/reducing firing atmospheres giving a characteristic gray/black color, and this is confirmed with the identification of maghemite in many of the sherds analyzed. The equivalent firing temperatures could be suggested to be around 750/950 °C considering also that the matrix is often optically active under the microscope. Previous studies on ERW1 (Madrid and Buxeda, 2008) suggested a firing temperature around 950/1000 °C for samples coming from Valencia. This opens the possibility of the existence of different products sharing a common general aspect but with different provenances and slightly different production technologies, but in a common pottery-making tradition.

On archaeological grounds, it is interesting to observe that, despite the relatively wide distribution of this ware, there seems to be a higher concentration inland than in coastal areas. In fact, in the Alicante and Murcia regions, the increase of ERW1 with the distance from the coast is clear. From an archaeological viewpoint the cooking pots in ERW1 were conceived to operate directly over the fire, following somehow a pre-Roman tradition. Instead, African cooking wares that will later invade the markets were rather used on a tripod or brazier (Bats, 1988; Aguarod, 1991; Arthur, 2007). Was this ware linked to areas where the substrate of the indigenous population was still strong? Were the production area/s and workshops located inland rather than in coastal areas and related to old indigenous settlements? Is the wider distribution inland related to a proximity of the production/s center/s? In this context, it is worth mentioning that some examples of ERW1 were used as votive materials in the rituals of foundation of buildings and as part of funerary practices (Quevedo, 2015), acquiring a meaning beyond their primary use as cooking wares.

## 6. Summary and conclusions

The analysis of ERW1 samples from Cartagena and Elche in southeastern Spain showed the presence of a major group including samples from both sites and indicating that the same ware produced in the same area was distributed to both sites. If the sample CAR-5 is classified as ERW1, then we should admit that there were various production areas preparing similar wares but using very different clays. This is also what previous studies by other researchers have suggested for the area of Valencia. If a multiplicity of production areas and/or workshops can be admitted, then ERW1 was not the product of a single production area but rather the result of a same pottery tradition or know-how, but perhaps with several workshops operating at the same time.

There are still many questions to be solved concerning this particular class of ware that was common in the southeastern Iberian Peninsula. The use of alumina-rich clayey materials certainly gave these ceramics excellent properties as cooking ware and this might have helped to have an important place in the markets in this part of Roman Iberia. Further research is still needed to define the different fabrics that can be associated with ERW1 and their provenance.

## Declaration of Competing Interest

The authors declare that they have no known competing financial interests or personal relationships that could have appeared to influence the work reported in this paper.

### *Acknowledgements*

This research was performed within the general framework of the activities of the Equip de Recerca Arqueològica i Arqueomètrica de la Universitat de Barcelona (ERAAUB), which is funded by the DIUE of the Generalitat de Catalunya (SGR 2017-01173). The study forms part of a larger project, *Archaeology, Remote Sensing, and Archaeometry: A Multidisciplinary Approach to Landscape and Ceramics from the Roman to the Medieval Period in Mallorca (Balearic Islands (ARCHREMOMOTELANDS)* (HAR2017-83335-P; PI Miguel Ángel Cau Ontiveros), funded by the Spanish Ministerio de Ciencia, Innovación y Universidades, with contribution by the European Regional Development Fund (ERDF). The contribution of L. Fantuzzi was developed within the framework of a Juan de la Cierva-Formación contract, also supported by the Ministerio de Ciencia, Innovación y Universidades.

We are most grateful to Miguel Martín Camino (Museo Arqueológico Municipal de Cartagena) for facilitating the sampling and study of the ceramic materials, to two anonymous reviewers for their helpful comments, and to Peter M. Day for English correction of the final text.

## References

Aguarod Otal, C., 1991. Cerámica comum romana de cocina en la Tarraconense. Institución Fernando El Católico, Zaragoza, Zaragoza.
Aitchison, J., 1986. The Statistical Analysis of Compositional Data. Chapman and Hall, London.
Aitchison, J., 1992. On criteria for Measures of Compositional Difference. Math. Geol. 24, 365–379.
Aldaya, F., García-Dueñas, V., 1972. Mapa Geológico de España, escala 1:200.000. Hoja 79: Murcia. Instituto Geológico y Minero de España, Madrid.
Arthur, P., 2007. Pots and boundaries. On cultural and economic areas between the Late Antiquity and the Early Middle Ages, in: Bonifay, M., Tréglia, J.-C. (Eds), LRCW 2. Late Roman Coarse Wares, Cooking Wares and Amphorae in the Mediterranean: Archaeology and archaeometry. Archaeopress, Oxford, pp. 15-28.
Baena, J., Álvarez, F., Aldaya, F., Navarro, F., Rodríguez, J., Santisteban, C., Elízaga, E., Goy, J. L., Zazo, C., Somoza, L., Bardají, T., Silva, P., 1993. Mapa Geológico de la Comunidad Autónoma de la Región de Murcia, 1:200.000. Instituto Geológico y Minero de España, Madrid.
Bats, M., 1988. Vaisselle et alimentation à Olbia de Provence (v. 350-v. 50 av. J.-C.). Modèles culturels et catégories céramiques. Revue archéologique de Narbonnaise 18 (1), 5-72.
Bermejo, J., Quevedo, A., 2014. The Fortuna Domus (Cartagena, Spain): An Archaeological Analysis of Household Activities in a Hispano-Roman Colonia. Eur. J. Archaeol. 17, 487–516.
Buxeda, J., 1999. Alteration and contamination of archaeological ceramics: The perturbation problem. J. Archaeol. Sci. 26, 295–313.
Buxeda, J., Cau, M.A., 2004. Annex I. Caracterització arqueomètrica de les produccions tardanes d'Iluro. Laietània 15, 449–498.
Buxeda, J., Kilikoglou, V., 2003. Total variation as a measure of variability in chemical data sets, in: Van Zelst, L. (Ed), Patterns and process: A Festschrift in honor of Dr. Edward V. Sayre. Smithsonian Center for Materials Research and Education, Washington DC, pp. 185-198.
Buxeda, J., Kilikoglou, V., Day, P.M., 2001. Chemical and mineralogical alterations of ceramics from a Late Bronze Age kiln at Kommos, Crete: The effect on the formation of a reference group. Archaeometry 43 (3), 349–371.
Cau, M.A., 2003. Cerámica tardorromana de cocina de las Islas Baleares. Archaeopress, Oxford, Estudio arqueométrico.
Cau, M.A., Fantuzzi, L., Tsantini, E., Burriel, J.M., Jiménez, J.L., Rosselló, M., 2019a. Caracterización arqueométrica de cerámicas comunes y de cocina tardoantiguas del asentamiento rural de L'Horta Vella (Bétera, Valencia). Sagvntvm 51, 215–232.
Cau, M.A., Fantuzzi, L., Tsantini, E., Ribera, A., Rosselló, M., 2019b. Archaeometric characterization of common and cooking wares from the Late Antique city of Valentia (Valencia, Spain). Archaeol. Anthropol. Sci. 11, 4035–4057.
Cultrone, G., Rodríguez-Navarro, C., Sebastian, E., Cazalla, O., De La Torre, M.J., 2001. Carbonate and silicate phase reactions during ceramic firing. Eur. J. Mineral. 13, 621–634.
Escrivà, V., 1995. Cerámica común romana del Municipium Liria Edetanorum. Nuevas aportaciones al estudio de la cerámica de época alto-imperial en la Hispania Tarraconenses, in: Aquilué, X., Roca, M. (Eds.), Cerámica comuna romana d'època Alto-Imperial à la Península Ibérica. Estat de la qüestió. Monografies Emporitanes 7, Ampurias, pp. 167-186.

Espinosa-Godoy, J. S., Martín-Vivaldi, J. M., Martín-Alafont, J. M., Pereda, M., Pérez, A., López, M. J., González, J. M., 1993. Mapa Geológico de España, escala 1:50.000. Hoja 977: Cartagena. Instituto Tecnológico GeoMinero de España, Madrid.

Fontboté, J. M., 1983. La Cordillera Bética: las zonas internas y unidades adyacentes, in: Comba, J. A. (Ed), Libro jubilar J.M. Ríos. Geología de España (Tomo II). Instituto Geológico y Minero de España, Madrid, pp. 251-343.

García-Rossell, L., 1973. Mapa Geológico de España, escala 1:200.000. Hoja 72: Elche. Instituto Geológico y Minero de España, Madrid.

Heimann, R.B., 1989. Assessing the technology of ancient pottery: the use of ceramic phase diagrams. Archaeomaterials 3, 123–148.

Hein, A., Müller, N., Day, P.M., Kilikoglou, V., 2008. Thermal conductivity of archaeological ceramics: The effect of inclusions, porosity and firing temperature. Thermochimica Acta 480, 35–42.

Hein, A., Tsolakidou, A., Iliopoulos, I., Momsen, H., Buxeda, J., Montana, G., Kilikoglou, V., 2002. Standardisation of elemental analytical techniques applied to provenance studies of the archaeological ceramics: an inter laboratory calibration study. Analyst 127, 542–553.

Huguet, E., 2012. Cerámica regional reductora de cocina altoimperial en la fachada mediterránea. In: Bernal, D., Ribera, A. (Eds.), Cerámicas hispanorromanas II. Producciones regionales. Servicio de Publicaciones de la Universidad de Cádiz, Cádiz, pp. 435–452.

Kretz, R., 1983. Symbols for rock-forming minerals. Am. Mineral. 68, 277–279.

Macias, J.M., Cau, M.A., 2012. Las cerámicas comunes del nordeste peninsular y las Baleares (siglos V-VIII): balance y perspectivas de la investigación. In: Bernal, D., Ribera, A. (Eds.), Cerámicas hispanorromanas II. Servicio de Publicaciones de la Universidad de Cádiz, Cádiz, Producciones regionales, pp. 511–542.

Madrid, M., Buxeda, J., 2008. Estudi de caracterització arqueomètrica de les ceràmiques de cocina altoimperials dels jaciments de les ciutats romanes de Valentia y Saguntum. Unpublished report, Universitat de Barcelona, Barcelona.

Maggetti, M., 1982. Phase analysis and its significance for technology and origin. In: Olin, J.S., Franklin, A.D. (Eds.), Archaeological Ceramics. Smithsonian Institution Press, Washington DC, pp. 121–133.

Maggetti, M., Neururer, C., Ramseyer, D., 2011. Temperature evolution inside a pot during experimental surface (bonfire) firing. Appl. Clay Sci. 53, 500–508.

Maritan, L., 2004. Archaeometric study of Etruscan-Padan type pottery from the Veneto region: Petrographic, mineralogical and geochemical-physical characterisation. Eur. J. Mineral. 16, 297–307.

Müller, N., Kilikoglou, V., Day, P.M., Vekinis, G., 2014. Thermal shock resistance of tempered archaeological ceramics. In: Martinon-Torres, M. (Ed.), Craft and science: International perspectives on archaeological ceramics. Bloomsbuty Qatar Foundation, Doha, pp. 263–270.

Pasqualini, M., 2009. Les céramiques communes de la Provence romaine. Fabrications locales et importations. IIe siècle avant notre ère / IIIe siècle de notre ère, in: M. Pasqualini (Dir.): Les céramiques communes d'Italie et de Narbonnaise. Structures de production, typologies et contextes inédits. IIe s. av. J.-C. – IIIe s. apr. J.-C., (Naples, 2-3 novembre 2006). Colléction Centre Jean Bérard, 30, Naples, pp. 157-164.

Pignatelli, R., Espejo, J., Crespo, A., 1973. Mapa Geológico de España, escala 1:50.000. Hoja 893: Elche. Instituto Geológico y Minero de España, Madrid.

Quevedo, A., 2013. La cerámica reductora de cocina de *Carthago Noua* (Cartagena, España), s. II-III d.C. In: Girón, L. (Ed.), I Congreso Internacional de Estudios Cerámicos, Homenaje a Mercedes Vegas. Servicio de Publicaciones de la Universidad de Cádiz, Cádiz, pp. 1065–1100.

Quevedo, A., 2015. Contextos cerámicos y transformaciones urbanas en Carthago Nova (s. II-III d.C.). Archaeopress, Oxford.

Quinn, P.S., 2013. Ceramic petrography. The interpretation of archeological pottery & related artefacts in thin section. Archaeopress, Oxford.

Raynaud, C., 2007. Les céramiques communes de l'Antiquité tardive en Gaule méridionale (IVe-VIIe s.). in: Bonifay, M., Tréglia, J.-C. (Eds), LRCW 2. Late Roman Coarse Wares, Cooking Wares and Amphorae in the Mediterranean: Archaeology and archaeometry. Archaeopress, Oxford, 247-262.

Raynaud, C., Elie, M., 2006. La céramique commune à pisolithes. Typologie, chronologie et diffusion (IVe–VIe s. ap. J.-C). Du Rhône aux Pyrénées: aspects de la vie matérielle en Gaule narbonnaise (fin du Ier s. av. J.-C.–VIe s. ap. J.-C.), Montagnac, 287-326.

Reynolds, P., 1993. Settlement and pottery in the Vinalopó Valley (Alicante, Spain): AD 400–700. Tempus Reparatum, Oxford.

Roberts, J.P., 1963. Determination of the firing temperature of ancient ceramics by measurement of thermal expansion. Archaeometry 6, 21–25.

Tendero, M., Ronda, A. M., 2014a. Ilici. I. La ciudad romana de Ilici, in Olcina, M. (Ed), Ciudades romanas valencianas. Actas de las jornadas sobre ciudades romanas valencianas. MARQ, Diputación de Alicante, Alicante, pp. 226-242.

Tendero, M., Ronda, A. M., 2014b. Nuevos datos sobre la Colonia Iulia Ilici Augusta (s. II-IV d.C.), in: Ramallo, S., Quevedo, A. (Eds), Las ciudades de la Tarraconense oriental entre los s. II.- IV d.C. Evolución urbanística y contextos materiales. Editum, Universidad de Murcia, Murcia, pp. 275-320.

Tendero, M., Ronda, A. M., Moreno, E., 2019. La cerámica en su contexto: análisis de un vertedero tardorromano en el margen noroeste de Ilici, in: Coll Conesa, J. (Coord.), Opera fictiles. Estudios transversales sobre cerámicas antiguas de la Península Ibérica, IV Congreso Internacional SECAH (Valencia 2017). Ediciones la Ergástula, Madrid, pp. 435-454.

Travé, E., Quinn, P., Álvaro, K., 2019. Another one bites the dust: quality control and firing technology in the production of medieval greyware ceramics in Catalonia, Spain. Archaeometry 61, 1280–1295.

Vera, J. A., 1983. LA Cordillera Bética: las zonas externas, in: Comba, J. A. (Ed), Libro jubilar J.M. Ríos. Geología de España (Tomo II). Instituto Geológico y Minero de España, Madrid, pp. 218–251.

Vera, J.A. (Ed.), 2004. Geología de España. Sociedad Geológica de España - Instituto Geológico y Minero de España, Madrid.

Whitbread, I.K., 1986. The characterisation of argillaceous inclusions in ceramic thin sections. Archaeometry 28 (1), 79–88.

Whitbread, I.K., 1989. A proposal for the systematic description of thin sections towards the study of ancient ceramic technology. In: Maniatis, Y. (Ed.), Archaeometry: proceedings of the 25th international symposium, pp. 127–138.

Whitbread, I. K., 1995. Appendix 3. The collection, processing and interpretation of petrographic data, in: Greek transport amphorae: a petrological and archaeological study. British School at Athens, Athens, pp. 365-396.